



HAL
open science

Structural modeling based on sequential restoration of gravitational salt deformation in the Santos Basin (Brazil)

Savio Francis de Melo Garcia, Jean Letouzey, Jean-Luc Rudkiewicz, André
Danderfer Filho, Dominique Frizon de Lamotte

► **To cite this version:**

Savio Francis de Melo Garcia, Jean Letouzey, Jean-Luc Rudkiewicz, André Danderfer Filho, Dominique Frizon de Lamotte. Structural modeling based on sequential restoration of gravitational salt deformation in the Santos Basin (Brazil). *Marine and Petroleum Geology*, 2012, 35, pp.337-353. 10.1016/j.marpetgeo.2012.02.009 . hal-01134814

HAL Id: hal-01134814

<https://hal.science/hal-01134814>

Submitted on 24 Mar 2015

HAL is a multi-disciplinary open access archive for the deposit and dissemination of scientific research documents, whether they are published or not. The documents may come from teaching and research institutions in France or abroad, or from public or private research centers.

L'archive ouverte pluridisciplinaire **HAL**, est destinée au dépôt et à la diffusion de documents scientifiques de niveau recherche, publiés ou non, émanant des établissements d'enseignement et de recherche français ou étrangers, des laboratoires publics ou privés.

Elsevier Editorial System(tm) for Marine and Petroleum Geology
Manuscript Draft

Manuscript Number:

Title: Structural modelling based on sequential restoration of gravitational salt deformation in the Santos Basin (Brazil)

Article Type: Original Research Paper

Keywords: Salt tectonics; section restoration; Santos Basin; passive margin; South Atlantic; deep offshore.

Corresponding Author: Mr. Sávio Francis de Melo Garcia, M.Sc.

Corresponding Author's Institution: Petrobras

First Author: Sávio Francis de Melo Garcia, M.Sc.

Order of Authors: Sávio Francis de Melo Garcia, M.Sc.; Jean Letouzey, PhD; Jean-Luc Rudkiewicz, PhD; André Danderfer, PhD; Dominique Frizon de Lamotte, PhD

Abstract: Structural restoration and basin modelling tools enable to evaluate complex sedimentary basins such as the ones extending along the South Atlantic Brazilian margin. Several structures result from a complex 3D evolution and most commercial algorithms usually consider vertical backstripping solutions, even when the basin evolution is controlled by gravitational instabilities and horizontal tectonic transport. Salt tectonics actually, promotes lateral gliding of the overlying sedimentary pile, whereas poor paleo-bathymetric data increase uncertainty and difficulty of any restoration. Cross-sections restoration is proposed, at first, to establish an easier understanding of the 3D geological complexities and to provide guidelines to handle more complex solutions. Two sections extending from the platform to deep waters of the Santos Basin, south-eastern offshore Brazil, have been chosen in areas where salt tectonics is simple enough to be solved by 2D restoration. These sections comprise both extensional and compressional deformation. Regional settings were important to establish the constraints applied on basic boundary conditions such as the overall paleo-bathymetry, the isostatic regional compensation, the salt volume control and the overall aspects related to structural style. Many restoration methods (simple shear, flexural slip and free methods) were used to restore the sedimentary deformation, including the salt gravity gliding. The 2D restoration results are consistent with five major sequences of sedimentary evolution: (1) the mechanical brittle pre-salt deformation, (2) the significant and fast salt deposition, (3) the initial post-salt deformation with predominant rafting tectonics, (4) the Late Cretaceous progradation sequence and coeval compressional evolution of minibasins, and (5) the Cenozoic sequence with less intense salt tectonics. A 1D subsidence analysis based on the 2D restored results is shown as a useful restoration control tool. The 1D results suggest a general proximal to distal filling controlled by salt tectonics. They also allow further discussion about areas with large horizontal gravity salt gliding.

Suggested Reviewers: Mark Rowan
Rowan Consulting, Inc., Boulder, CO
mgrowan@frii.com
He has work for a long time with the paper subject

Bruno Vendeville

Université Lille 1
bruno.vendeville@univ-lille1.fr
He has work with salt tectonics

Chang H Kiang Ph.D
Professor, Geologia, Universidade Estadual de Rio Claro
chang@rc.unesp.br
He is one that knows well the Santos Basin.

John R Underhill Ph.D
Professor, Chair of Stratigraphy, University of Edinburgh
jru@staffmail.ed.ac.uk
Underhill supervised the Ph.D thesis of Marta Guerra, 2008, also about the Santos Basin.

Research Highlights

We reconstructed the evolution through time of two sections in salt complex area.

The restoration shows the geometry of 14 steps from Aptian to present.

Our approach integrates isostasy, bathymetry and deformation mechanism as constraints.

Regional depositional constraints & 1D analysis made a complementary calibration tool.

Results showed a progradation over thick salt layer deposited on pre-existing relief.

1. Introduction

1
2 Salt tectonics is one of the most complex deformation processes operating in sedimentary basins. For instance, there is
3
4 no unique nor simple solution to restore complex structural sections involving salt tectonics. Most current methods of
5
6 sequential restorations, however, are based on geometrical approaches imposed to the geological events. Several gross
7
8 and poorly controlled simplifications are generally required to simulate such mode of deformation, not really integrated
9
10 with geological process and properties, limiting applicability and effectiveness of the restoration methods.
11
12 The study area of the present work in the Santos Basin was intensely deformed by salt tectonics. This passive margin
13
14 basin constitutes the southernmost prolific petroleum basin of the South Atlantic Ocean which was developed over
15
16 stretched continental crust in eastern offshore Brazil (Fig. 1). The deep offshore part - close to the study area - constitutes
17
18 a new frontier for petroleum exploration. The wide bathymetric expression of the Santos Basin was developed over a
19
20 thick salt layer, a fundamental element to the evolution of the basin history. Considering differential properties like density
21
22 and compressibility between evaporites and other sediments, numerical tools are needed to control decompaction
23
24 restoration and flexural isostatic compensation.
25
26 Several authors such as Guerra (2008), Rouby et al. (1993) and Szatmari and Demercian (1993) have discussed the
27
28 basin evolution using restoration methods. Cobbold et al. (2001), Meisling et al. (2001) and other authors also interpreted
29
30 the complex thin-skinned deformation above the Aptian salt in this basin using structural analyses and regional
31
32 interpretation. More recently, a failed sea floor spreading in the southern portion, an outer high located over the São
33
34 Paulo Plateau and the overall basement compartmentalization of the basin evolution were described in several papers
35
36 and presentations such as Braga et al. (2003), Carminatti et al. (2008) and Scotchman et al. (2006).
37
38 In this work, a comprehensive restoration technique based on data and tools integration to minimize the strong impact of
39
40 simplifications on basin evolution results is applied. The workflow also counts on geologic models in order to guide and to
41
42 constrain the restoration assumptions. It marks the structural modeling character of this work: not just a technique
43
44 application but an idea development.
45
46 A relatively simple 2D workflow based on classical backwards cyclic steps is carried out here: (1) isostatic flexural
47
48 response to unloading and decompaction; (2) modular fault-related restoration to fit a paleo-bathymetric constraint (a
49
50 morphologic model supported by well and seismic data); and (3) adjustments in the salt layer, under conservative volume,
51
52 integrating the bathymetric and isostatic results.
53
54 Complementing, the 2D restoration is revisited through 1D complementary analysis, which can be used as a calibration
55
56 modeling tool, producing more consistent structural scenarios. The workflow developed in the present work intends to be
57
58 the most rigorously integrated and interlaced as possible, marked by suitability or rightness of the tools and methods
59
60 applied. It could be applicable in other basins and complex situations.
61
62
63
64
65

2. Geological setting

1
2
3
4The Santos Basin constitutes a good example of continental drifting. It results from an asymmetrical partition of the
5
6Gondwanian “super-continent” whereby the Brazilian marginal basin became wider than its conjugate African basin. The
7
8Santos Basin extends over 352,000 km² down to 3,000 m water depth. The current knowledge of its architecture comes
9
10from just over one hundred wells and numerous 2D and 3D seismic surveys. It is bounded in the northeast by the Cabo
11
12Frio High and in the southwest by the Florianópolis Platform (Fig. 1). The studied area outlined by the red polygon covers
13
146,000 km².

2.1 Stratigraphy

15
16
17
182.1 Stratigraphy
19
20
21
22The Santos Basin development can be described by successive evolutionary phases, including its pre-rift evolution, and
23
24subsequent rifting and drifting episodes. The stratigraphic description presented herein (Fig. 2) is in agreement with the
25
26general description of Carminatti et al. (2008) and the stratigraphic chart proposed by Moreira et al. (2007). A maximum
27
28sedimentary thickness of approximately 12,000 meters was deposited in the Santos Basin depocenters (Pereira and
29
30Macedo, 1990).

31
32The basin opening started about 135 Ma ago, with a 20 Ma-long period of continental breakup and rifting (Moreira et al.,
33
342007; Pereira et al., 1986; Pereira and Feijó, 1994). A thermal intracratonic dome developed in the Late Jurassic. Its
35
36collapse and coeval rifting occurred in the Early Cretaceous, leading to the opening of the South Atlantic Ocean (Williams
37
38and Hubbard, 1984).

39
40Pre-salt sequences of syn-rift and post-rift phases are included in the Guaratiba Group. The syn-rift sequence is
41
42composed of significant basaltic volcanism followed by continental sedimentation in half-grabens formed by block rotation
43
44and faulting processes. A major unconformity separates the overlying post-rift Late Aptian sequence, which was
45
46deposited at a time when the fault system was less active than during the deposition of older units. The Late Aptian
47
48sequence is composed of carbonates and shales typical of a transitional environment from continental to shallow marine.
49
50Although Moreira et al. (2007) postulated a post-rift stratigraphic position to this package, in disagreement with previous
51
52authors such as Pereira and Feijo (1994), this controversy has no implication on the restoration approach carried out
53
54here.

55
56The Aptian Salt sequence recorded by the Ariri Formation is about 2,500 m thick on average. This salt formation was
57
58quickly and unconformably deposited above the Aptian syn-rift limestones during the transition from continental to
59
60oceanic conditions. It extends across the West African and Brazilian continental lithospheres (Karner and Gamboa,
61
62
63
64
65

2007), and was deposited under a high sedimentation rate in the order of 1 km over a period of 500,000 years (Dias, 1998). The age of the salt is still controversial. It has been attributed either to an early post-rift phase at the onset of oceanic spreading (Davison 2007; Gamboa et al., 2008; Henry et al., 1995; Jackson et al., 2000; Marton et al., 2000) or to a late syn-rift stage, being then the last deposits before the onset of oceanic spreading (Karner et al., 2003; Ian et al., 2009).

The drift phase is subdivided into three major sequences, i.e. the Camburi, Frade and Itamambuca groups (Fig. 2), which record the Albian to Cenomanian sequences, an intervening Late Cretaceous progradation episode, and the Cenozoic sequence, respectively. These subsequent post-salt sequences are deformed by gravity-driven tectonics with non-homogeneous displacements along the basin (Assine et al., 2008), mainly due to heterogeneities of the salt thickness and detachment surface, as well as to a progressive tilt of the basement.

The Albian to Cenomanian sequences of the Camburi Group include the first deposits clearly related to the drift evolution after deposition of the evaporites. Proximal siliciclastics, shallow-water limestones in the continental shelf, and marls and shales in the distal basin were deposited during the Albian. The overlying Cenomanian sequence records the onset of a retrogradation pattern which accounts for the major marine transgression in the Santos Basin and culminates with the Turonian anoxic OAE-2 event (Arai, 1988). Most of the Late Cretaceous siliciclastic progradation sequences were deposited in continental paleo-environments, pushing the continental shelf limits towards the most distal portions of the basin. After a strong erosional episode in the Santos Basin, a basinwide regressive episode gradually shifted the coastal line eastward for about two hundred kilometers near the Cretaceous-Cenozoic boundary, building a wide progradational wedge. The Cenozoic sequences are marked by decreasing salt tectonics and a high frequency of sea level variations. An important sea-level fall is associated with the Paleocene series which presents thin sedimentation in the central part of the basin, probably due to reduced accommodation space and growth of salt structures (Assine et al., 2008). A new progradation cycle during the Early Eocene accounted for the shelf break migration towards the basin, followed by aggradation periods during the Late Eocene. A new transgressive trend developed above an Early Miocene unconformity, recording the largest sea-level change of the Neogene period. The Late Miocene began with a global eustatic fall (Gradstein et al., 2004; Moreira et al., 2007) and erosional events correlated with glaciation periods. The last and most recent sediments in the Santos Basin are evolving from proximal sandstones to distal diamictites and muddy wedges.

Based on the stratigraphic chart of Moreira et al. (2007), fifteen horizons were interpreted on the 2D seismic sections. These horizons have been used to build two structural sections (Fig. 3), which are about 120 km long and less than 20 km apart. These sections have been subsequently used as input data for the 2D structural restoration analysis, with special attention to the salt tectonics.

2.2 Structural framework

The São Paulo Plateau constitutes a major deepwater physiographic feature within the Santos Basin. This wide domain, already studied by many authors (Masclé and Renard, 1976; Kumar et al., 1977; Cande and Rabinowitz, 1978; Guimarães et al., 1982; Demercian, 1996; Cobbold et al., 2001; Gomes et al., 2002; Scotchman et al., 2006, Carminatti et al., 2008), developed over an extensively stretched continental crust still attached to the Brazilian margin. The evolution of this plateau is intricately correlated to the overall dynamics of the South Atlantic margins.

Ductile heterogeneities in the basement framework have controlled the evolution of the basin through time. Long NE-trending lineaments have been mapped onshore, and can also be clearly observed in the offshore by means of magneto-structural imaging, at least as far as the Cretaceous hinge line (Braga et al., 2003). Reactivations of these lineaments and coeval shear zones controlled both the formation of the coastal ranges (i.e., Serra do Mar and Serra da Mantiqueira) since the Coniacian (e.g., Almeida, 1976), and the compartmentalization of the offshore basin.

Inherited from the initial rifting complexity, an aborted proto-oceanic domain has been described in the southern part of the São Paulo Plateau (Carminatti et al., 2008; Gomes et al., 2002; Gomes et al., 2009; Meisling et al., 2001; Scotchman et al., 2006). It is observed as a triangular shape of shallower bathymetry in gravity and magnetic maps (Mohriak, 2001). The NE-trending aborted rift propagated northward, making possible to extend laterally this feature up to coeval pre-salt normal faults in the proximal part of the study area (Fig. 1). Although available or published data are limited in the Santos Basin, we assume that its overall crustal thinning, including this aborted rift branch, is similar to the Lavier and Manatschal's model (2006) involving an H block in front of a V-shaped basin (Fig. 4). This crustal thinning evolution, which is broadly distributed in the upper crust and probably reflected basin compartmentalization by shear zones, has been studied in more details by Zalán et al. (2009).

The current target for petroleum exploration, known as "the Outer High of the Santos Basin" (Gomes et al., 2002) or the Santos External High" (Carminatti et al., 2008), is located a bit farther to the southeast of the studied area, in the compressive domain. It is an important basement structure in the central part of the São Paulo Plateau. This regional high hosts the recent oil discoveries and the most important plays of the Santos Basin, with a recovery potential of 60 billion barrels of oil equivalent (Carminatti et al., 2008; Gomes et al., 2009). In the Santos External High area, beyond the study area, the marine sequence record is relatively thinner, with a thickness in the order of 1,000 meters. As attested by recent wells, Aptian carbonate reservoirs were deposited over this wide basement high in shallow-water marine environments (Carminatti et al., 2008). Beyond a shelf break, interpreted as the eastern limit of the carbonate buildup, deeper waters occurred. More restricted and shallow depositional environments are expected to develop west of this paleo-high due to the presence of an older salt layer. The understanding of the calcareous facies succession of the pre-salt sequence of the Santos External High is a major exploration challenge.

2.3 The importance of evaporites

1
2 The Santos Basin is the southernmost Atlantic basin where Aptian evaporites were deposited. Climatic conditions were
3
4 favorable for salt deposition over the São Paulo Plateau and other basins to the north. These conditions were enhanced
5
6 by the structural alignment of paleo-highs such as the Florianópolis Platform and the São Paulo Ridge (Fig. 1). The highs
7
8 acted as an efficient barrier at the southern limits of the basin that blocked the marine water circulation derived from the
9
10 proto-Atlantic Ocean extending farther south during the Aptian salt deposition. Simultaneously, the Santos External High
11
12 blocked the marine waters coming from the east. A fast (ca. 0.5 Ma) isostatic subsidence of probably more than 1,000 m
13
14 was induced by the deposition of the thick salt layer. Nevertheless, the existing tectonic barriers blocked the entrance of
15
16 the surrounding oceanic waters and kept the basin sufficiently closed to account for salt deposition.
17
18 Evaporites can flow like a viscous material when they become loaded by sediments. The salt tectonics occurs between
19
20 the Cretaceous Santos hinge line in the west and the salt pinch-out in the southeast, close to the São Paulo Ridge. They
21
22 have been deformed and account for the regional spreading and gliding of the overlying sedimentary cover since the
23
24 earliest depositional stages of the Santos Basin (Demercian, 1996). The high post-Aptian accumulation rates above the
25
26 thick Aptian salt sequence produced a relatively shallow bathymetry over the São Paulo Plateau. During the drift phase,
27
28 both the salt and its overlying sedimentary cover were intensely deformed, resulting in a convergent radial gliding
29
30 configuration (Cobbold and Szatmari, 1991), with increasing contraction from the coast towards the distal highs. The most
31
32 active tectonic stage was the Late Cretaceous, as a response to the loading of progradation wedges over the thick salt
33
34 layer.
35
36 The Cabo Frio Fault marks the transition from a dominantly extensional to a rather compressive salt tectonic domain
37
38 (Mohriak and Szatmari, 2001). The classical minibasins, developing piggyback of the compressive gravity-driven domain
39
40 beyond this fault, seems to result from a sedimentary bypass through the slope.
41
42 Within the São Paulo Plateau, one of the most significant preserved stratified salt columns is located over the Santos
43
44 External High (Freitas, 2006). This package is not really autochthonous, as it has been laterally displaced above the basal
45
46 detachment during the development of the underlying basement relief. More rugged features observed on section A-A'
47
48 can be related to the preexisting structural framework, differentiated between the sections A-A' and B-B' (Fig. 3).
49
50
51

52 3. Methods

53
54
55
56
57 The restoration procedure presented here is based on the following backwards successive steps: (1) sediments removal
58
59 and decompaction with isostatic flexural compensation; (2) fault-related and salt movement restoration fitting the paleo-
60
61 geometry to a reference target; (3) final paleo-bathymetric adjustments. Compared with other restoration methods (e.g.
62
63
64
65

Rowan, 1993), this restoration is a simplified derivation which simultaneously considers a flexural isostatic compensation and a vertical decompaction procedure. In addition, it does not consider any direct control, data about eustasy or thermal cooling. All effects of these processes are compensated in the final paleo-bathymetric calibration. Fault-related and salt movement deformations are restored in traditional handmade transformations considering a conservative mass balance for the sedimentary layers, including the ductile salt, and a defined paleo-geometry (shelf-slope-rise) with a coherent structural style of salt deformation. This restoration solution method is performed on RECON-MS, a Petrobras in-house software.

Backstripping with flexural isostatic compensation – Due to compaction laws, the layer decompaction solution with isostatic correction requires a detailed facies definition along the entire section. Only the salt layer is considered not compressible during the decompaction step. Once the uppermost sedimentary layer is removed, the decompaction of the underlying layers due to the removal of its overburden is a discretized calculation along the section. All the remaining decompacted units are referenced to the base of the removed unit. Once the decompaction is done, isostatic compensation with a crustal flexural deformation component is calculated. This procedure can be found (including improvements) in other specific applications (e.g. Roberts et al., 1998). This isostatic approach needs a supplementary paleobathymetry calibration data to fit the real equilibrium. The magnitude of isostatic flexural deformation depends on the applied sedimentary load as well as on the flexural properties of the crust that undergoes the deformation. An unloading approach considering only a local Airy-type backstripping history cannot approximate regional isostasy (Bender et al., 1989; Karner, 1982; Roberts et al., 1998; Watts et al., 1982).

The sections length (around 120 km) does not represent the entire sedimentary basin load (which extends over more than 400 km beyond the study area), thus producing a narrower isostatic unloading than it really should be. The post-salt sequence becomes progressively shortened in the study area during the sequential restoration of the salt gravitational gliding, which means a similar loss in the representativity of the load. An additional sedimentary load is required in the sections in order to compensate the loading representativity and further border effects. It is needed to simulate the regional extent of the basin as well as to restore in the initial sections the missing portions of the sedimentary cover and of the initial salt layer, which have been subsequently translated outside of the model. The lateral continuity of the Aptian evaporitic sequence (more than two thousand meters thick) towards the Santos External High (Carminatti et al., 2008; Gomes et al., 2009) (Fig. 5) make this lateral insertion of sedimentary section a reasonable assumption.

3.1. Modular restoration

To restore the original features of each section, the applied algorithms retain length or area of layers respecting the volume conservation law. Thus, neither gain nor material loss impacts the resulting geological features over time.

Considering dominant ductile deformation for the salt layer and brittle deformation for other sediments, whenever needed, the section has been subdivided every restoration cycle into minor individual modules with a similar deformation process.

1
2 These modules are limited by well defined geological elements such as stratigraphic contacts, salt diapirs borders, sea
3
4 floor and/or normal faults. Each module is restored by geometrical transformations in order to better fit the target
5
6 geometry (reference paleo-bathymetry) and lateral module boundaries (faults, diapirs or section borders). We have used
7
8 here the simplest methods to obtain simple restoration solutions. The solution implemented for the simple shear
9
10 transformations in the software is able to preserve the modules' areas on the 2D restoration results. These shear
11
12 transformations were used to restore brittle modules in the extensional deformation domain and also in less deformed
13
14 situations of the distal domain. Flexural unfolding transformations preserving length on the template bed direction and
15
16 parallel to the unfolding axes were preferentially used to restore most of the folded minibasins modules. Considering that
17
18 the major deformation is concentrated close to the faults and diapirs flanks, sometimes partial restoration steps were
19
20 superimposed, increasing shear restoration rates to better restore some intensely deformed borders. Sometimes part of
21
22 the salt diapir was included in the module to smooth the rugged fault or diapir geometries. All these operations could be
23
24 similarly reproduced with any commercial restoration software.

25
26 In contrast with other brittle sedimentary rocks, the ductile rheology of the salt layer was treated by free adjustment to
27
28 other restored modules. The salt layer thickness was modified to conform the differential deformation between its
29
30 overlying and underlying layers. The degree of freedom of this salt operation was established by structural coherence, a
31
32 factor discussed further below, always respecting the limits of the restored overburden. A constant amount of salt is an
33
34 approximate hypothesis applied only under this overburden. Along the whole section, it is not a reliable hypothesis for the
35
36 three-dimensional gravitational gliding of the study area. The lateral "void" created due to the lateral shortening of the
37
38 restored extensional domain is filled as explained before.

42 3.2. Paleo-bathymetric referential geometry

43
44
45
46 The 2D restoration approach requires paleo-bathymetric profiles at each incremental step to which the basin-driving
47
48 subsidence should be adjusted. The Santos Basin is characterized by a wide and shallow continental margin made up of
49
50 a thick wedge produced by high accumulation rates of sediment gliding above the Aptian salt. This margin has a
51
52 particular development in the basin – 700 km offshore – decreasing the brittle sedimentary thickness over distal portions
53
54 of the São Paulo Plateau. The margin development allows to interpret an evolution with gradual changes on the shelf /
55
56 slope / rise geometry, always controlled by highs at the distal positions.

57
58 The shelf / slope / rise limits can be recognized by their general characteristics. The continental shelf domain is an
59
60 extended, flooded and almost flat perimeter of the continent associated with the coastal plain, with a water depth usually

61
62
63
64
65

limited to 200 m (Pinet, 1996). In the case of the Santos Basin continental shelf, it is exceptionally wide (in the order of 200 km). The shelf ends when the slope gradient abruptly changes at a point called shelf break. This point was quite easy to interpret in the seismic sections for the different post-salt interpreted horizons. Beyond this gradient break, the average gradient of the continental slope is 3°, with a maximum value of 10° (Gross, 1972). The transition to the continental rise is marked by another gradient change at the foot of the continental slope, beyond which a sedimentary pile was still depositing. The topographic gradient of the continental rise is intermediate between the previous domains, in the order of 0.5-1°. In the Santos Basin, it merges with the deeper oceanic part of the abyssal plain through the São Paulo Ridge topography.

The shelf break and the foot of the continental slope were interpreted for each different horizon on the 2D seismic data in the study area (Fig. 6), as well as their general paleo-geometry position through time. These points provide key references for the shelf / slope / rise target geometry during the restoration of modules. The final geometry was ultimately calibrated by the available paleo-environment data from wells. Additional uncertainties can be considered about the proximity and possible similarity of the shelf break point with the axis of the Cabo Frio roll-over fault. The basal points called foot of the continental slope are always located on the hangingwall of the Cabo Frio Fault in the study area. Every individual decompacted module has been restored to fit the target geometry of the restoration timing as a first approximation. Some difficulties arise to adjust the isostatically decompacted layers to this target geometry. They will be accommodated through the salt layer restoration and, eventually, local isostatic adjustments in the brittle pre-salt set. It is important to remember that both thermal-subsidence and eustatic processes are not considered in the calculations, but they will be compensated by the paleo-bathymetric calibration.

3.3. Structural consistency

The most important criterion for the restoration concerns the structural consistency. The structural evolution from salt deposition to present time results from gravity gliding and progradation above a thick and ductile salt layer. The extensional features occur in the proximal parts of the sections, i.e. in the platform and upper slope domains. Compressive gravity-driven structures and the minibasins development are restricted beyond the toe of the continental slope, where relatively thinner post-salt layers are observed. During the gravity gliding deformation, the thick salt layer gradually becomes more deformed. Once the layer is locally depleted or welded, either in the footwall of the extensive growth faults, or in the compressive domain below some minibasins, both the overburden and salt thicknesses must be consistent with the paleo-bathymetry. This must be checked every restored cycle. If erosion features observed on the slope domain are interpreted as a local restriction for accommodation and/or sediment bypass, no major thickness variation would be expected at these positions

in the salt layer restoration. On the other hand, if a thicker layer is deposited after salt withdrawal, either due to local collapse or gravity slide, this shift must also be consistent with the paleo-bathymetry in the salt layer restoration.

1
2 If salt thickness variation is required through time, certain features should be avoided, i.e. the successive random-looking
3
4 opening and closing of salt windows as well the random increase and decrease of the salt thickness. In all these
5
6 situations, the local subsidence rates applied to brittle layers and deformation rates of the underlying ductile salt layer
7
8 should be consistent with the bathymetry variation.

9
10 Figure 7 shows a detailed restoration example of the cyclic applied methodology. These restoration steps include:

11
12 I) The initial (present day) condition of the section A-A';

13
14 II) The decompaction of the most recent layer with flexural isostatic compensation;

15
16 III) First paleo-bathymetric approximation, indicated by the dashed line based, in this case, on the present day bathymetry
17
18 which is represented by the blue line. Both lines were superposed on the top of the decoupled post-salt package. This set
19
20 is decoupled of the pre-salt package, once the salt layer had been suppressed. Small circles show two salt windows that
21
22 should be preserved;

23
24 IV) Adjustments of the post-salt package to the top target dashed line by geometric operations opening locally a larger
25
26 space for the salt layer. A circle shows the least adjusted point;

27
28 V) Final adjustments required to better replace the initial amount of salt below the post-salt package. This step leads to a
29
30 completed restoration cycle.

31
32
33
34 4. Restoration and discussion

35
36
37
38 Fourteen different restoration outcomes are presented as restoration results for the geological evolution of fifteen
39
40 interpreted horizons in the two sections, A-A' and B-B'. These results were obtained following the procedure already
41
42 described above. The older three restoration outcomes are related to deformation of the pre-salt sequence when brittle
43
44 tectonics was prevalent. They are strongly different from the other eleven restoration cycles which are recording the
45
46 effects of thermal subsidence and ductile salt deformation. The pre-salt sequence is the first of five major sequences
47
48 considered in the structural evolution to account for the different observed architectures. The subdivision of the post-salt
49
50 sequences can be explained by the major factors controlling salt tectonics: the preexisting relief at the salt deposition time
51
52 and the sedimentation rate.

53
54 They provide different conditions of instability for the gravitational gliding and also different ratios of thickness between
55
56 the salt layer and its overburden through time. These various aspects of salt tectonics have been already well discussed
57
58 by several authors (e.g., Cobbold and Szatmari, 1991; Weijermars et al., 1993; Lerche and Petersen, 1995; Garcia, 1999;
59
60 Mohriak and Szatmari, 2001; Hudec et al., 2009).

61
62
63
64
65

The five sequences are described below.

4.1. Pre-salt sequence

The quality of the subsalt seismic imagery is not good enough here to solve uncertainties related to the pre-salt layers. In general, the tilted blocks involving the basement and synrift strata beneath the base of the salt were defined only by few faults without any good definition of the dipping attitude of infra-salt series (Fig. 8).

The observed unconformities are not well mapped continuously either, and no data about the target relief for these sequences are available. The restoration for these sequences was strongly marked by rotation and an important extension is observed in the proximal deep basement domain. This latter feature is consistent with the hypothesis of a northward lateral prolongation of the brittle normal structures described earlier farther south in the failed spreading centre (Fig. 1). It seems also possible that this structural low was already formed before the salt deposition time. The geometry at the restored scenario of the pre-salt sequence top predates the conditions to the salt deposition. However, the lack of bathymetric data prevents any secure calibration and therefore, this geometry remains quite speculative, resulting only from the isostatic and structural adjustments applied during the restoration. Ultimately, the pre-Aptian basement architecture is assumed here to have been less deformed than the present-day architecture of the pre-salt layers derived from the interpretation of seismic images.

4.2. The Aptian Salt sequence

The salt layer glided progressively toward the deeper centre of the basin, due to gravitational instabilities (Fig. 9). The light pink portion of the salt layer represents the amount its restored movement. In the study area, a very heterogeneous salt layer presents different average thickness in each section: it is around 1,600 m-thick in section A-A' and only about 700 m-thick in section B-B'. A large amount of salt was pushed toward the distal portions of the basin, outside of the study area. However, this salt still must be taken into account when restoring the sections. Due to the strong isostatic compensation response, part of the basement tilting was modified in order to generate enough accommodation space and to restore a more homogeneous salt layer over the preexisting rift geometry. The resulting salt layer thickness is about 2,800 m for section A-A' and about 1,200 m for B-B'. These differences were due the initial rifting geometry but also due to isostatic differential effects in both sections. A very smoothed yet not flat geometry was proposed here for the top of the restored salt layer at its deposition time. Considering the available seismic data and the significant superimposing effects of a continuous salt deformation, it was not possible to interpret any structural feature deforming the Aptian salt before deposition of the clastic and carbonate overburden units.

4.3. Albian to Cenomanian sequences

1
2
3
4 The first post-salt sequences include the deposition of Albian carbonates and part of the Late Cretaceous marine
5
6 siliciclastics. These sequences involve several fault-separated modules with gaps of several kilometers in both sections,
7
8 including some uncertainty about their extent in some intermediate modules (Fig. 10). The simply deformed modules
9
10 document the large magnitude of raft tectonics operating at the onset of halokinesis. The great salt volume associated
11
12 with a still thin overburden favours a fast gravitational gliding of the latter, resulting in lateral gaps where the Albian-
13
14 Cenomanian cover was progressively displaced. Different sedimentation domains and paleo-environments were linked
15
16 with the shelf / slope / rise geometries, respectively. A relatively thick salt layer is interpreted in the shelf / slope portions
17
18 whereas thin and folded sediments are observed in the rise domain.
19
20 The thickness variations interpreted in the seismic data for the Albian and Cenomanian layers show a thick proximal
21
22 portion developed in continental shelf and slope domains. An underlying thick salt layer provides the initial minimum basin
23
24 amplitude to accommodate the carbonate shelf development. Thin and folded distal Albian carbonates interpreted as
25
26 continental rise deposits are clearly restored in their initial folding stage and reconnected at their correct paleo-
27
28 bathymetric position (Fig. 11). In the next steps, still before the development of the classical minibasins, they were
29
30 translated eastward by the rafting tectonics. The carbonates thickness variations resulted in a differential rheology
31
32 pattern, which controlled the Cabo Frio Fault development. Restoration results suggest that the Cabo Frio Fault evolution
33
34 is correlated with the progradation of the thicker overburden and the squeezing of the salt towards the thinner portion of
35
36 the basin located at the local structural high currently observed in the middle of the sections.

4.4 Late Cretaceous progradation sequences

41
42
43
44 During the massive progradation of the Upper Cretaceous, the salt movement has built multiple overburden
45
46 compartments limited by faults or salt structures (Fig. 12). The proximal area is initially characterized by a thicker post-salt
47
48 package, already compartmented by diapirs with antithetic tendency in a restricted area behind the foot of the slope. The
49
50 slope advances as a consequence of the progradation event and seems to control the Cabo Frio Fault development since
51
52 its onset. Structural and thickness differences among these Late Cretaceous restored outcomes are observed in both
53
54 sections, denoting the complex evolution of the progradation in the hanging wall of the Cabo Frio Fault. The general
55
56 antithetic tendency is not clearly noted in part of section A-A'. A significant basinwards retreat of the Cabo Frio footwall is
57
58 restored and little or no fault gap will remain to be restored in subsequent phases. Major depocenters can be easily noted
59
60 beyond the continental shelf. The minibasins became more developed during this progradation. Such regional shift of the
61
62
63
64
65

sedimentation pattern was already described by Assine et al. (2008). The location of these depocenters is probably controlled by a bypass through a continental shelf blocking against the local structural high, and by a local ramp adjustment in the Cabo Frio Fault. Initial salt windows are formed beneath locally thick post-salt depocenters.

4.5. Tertiary sequences

The top and most recent layers are the least deformed (Fig. 13). They present limited deformation compared to the final stages of salt tectonics. These layers were deposited under moderate sedimentation rates, not enough to induce significant thickness variation or salt deformation. The post-salt overburden is already very thick and there are many welding points and salt windows to block the salt gliding.

The Cenozoic evolution was the easiest to restore within the study area. However, the isostatic response shows very limited accommodation space near the slope domain, close to the salt growing structures where local thickness variation and small erosional traces are observed in seismic data (Fig. 14, detail 1). If these constraints point uncertainties about the isostatic parameterization, they also invoke some compression due to squeezed underlying salt structure. The erosion features on the Miocene horizon produce diagnostic roughness on the horizon surfaces that can be smoothed in order not to transfer them downwards. Ongoing activity of fold growth associated with the salt diapirism at the borders of the minibasins beyond the Cabo Frio Fault cause the uplift and erosion of the adjacent flanks of the minibasins (Fig. 14, detail 2).

4.6. Isostasy

Applied as lower boundary conditions to the sedimentary layers below the salt during restoration, the calculations for the flexural isostatic compensation consider the entire loads applied to the mantle by the basin infill and crust. A potential crustal weakness in the Santos Basin was considered with values of 5 km for the effective elastic thickness and 2.78 g/cm³ for crustal density along the whole section and during all the geologic time. The crustal thinning can be estimated by horizontal stretching or synrift sedimentary loading as in the models of McKenzie (1978), Wernicke (1981), or by formation of weak ductile shear zones as in the model of Lavier and Manatschal (2006), but no specific study has been done to measure these parameters that were arbitrarily assigned. These are sensitive parameters. Using them, it is possible to note gentle undulations with amplitudes of up to 50 meters high on the isostatic compensation results, in phase with the paleo-environmental adjustments required to restore the sections. On the other hand, if we use values of 20 km for elastic thickness and 3.33 g/cm³ for crust density, for example, then the flexural isostatic compensation for the removal of the upper layer (the most recent sediments) would be 18 % deeper. In contrast, the heterogeneities of diapirs,

minibasins and growth faults with a wavelength of a few tens of kilometers would not cause any noticeable differential isostasy at the scale of the restored sections. One simplified and homogeneous crust with a single elastic thickness through space and time can also be unrealistic given the basement rheological heterogeneities. Moreover, the crustal elastic thickness could vary with both its physical integrity and with the thermal regime to which it is submitted. Difficulties to set the restored scenario into the bathymetric limits established by data and the isostatic response can be observed on the results, mainly in restoration cycles comprised between Eocene to recent times (Figs. 13 and 14). According to the restoration progression in the earlier stages (from Albian to Maastrichtian), even if the salt tectonic is more intense, a thicker salt layer gives more freedom to restore and adjust the restored paleo-bathymetric model. An important limitation of the restoration tool is the fact that no isostatic effect for the repositioned restored sedimentary masses is recalculated. This can be observed in the isostatic magnitude of the restored Cenomanian outcome for section B-B' (Fig. 10) where the isostatic response to the removal of the first progradational deposits (Fig. 12, dark orange layer) is noted in the basal geometry of the restored Cenomanian outcome, without any recalculated effect of the thicker restored salt layer. The more layers are interpreted or interpolated in a section, the more this isostatic deviation could be minimized, i.e., shorter time intervals from one restoration phase to the other represent more frequent repositioning and smaller lateral transfers of restored masses. However, the effect remains in the accumulated result.

4.7. Bathymetry

Applied as upper boundary condition to every post-Aptian restoration cycles, the bathymetry model proposes target geometries with low resolution (according to the available data). The uncertainties in the bathymetry model are represented by large intervals of time and wide ranges of water depth (Fig. 15). In the deeper portions and for several restoration cycles which have no data available, the bathymetric model was freely extrapolated. A critical point was found at the evaporites deposition time. The model assumes a preexisting low, not invaded by oceanic waters, since the isostatic effect produced by the thick salt layer requires additional space so that its fast and continued deposition does not create positive relief (there is no salt deposition on mountains). For the older units, deformed under a rifting tectonic regime, there are no paleo-environmental data for calibration and irregular reliefs were produced by the restored rotated blocks. It is not sufficient to draw the preexisting low geometry (Fig. 8). The problem is obvious in the 1D subsidence geohistory graphics discussed ahead.

4.8. Structural restoration style

Applied throughout the section to all restored cycles after salt deposition, a solution to the lateral movement of masses due to the salt gliding takes into account different limitations for bathymetry and isostasy in each situation. This handmade solution aims at a structural coherency through time so that there are no observed alternations of thickness or controversial structural inversions. Intense salt deformation starts from an initial scenario with more homogeneous salt thickness, with longer wavelength for domes and diapirs while overlapping clastic sediments partially expel the underlying salt. All positive reliefs of salt were cut and compensated in the restored salt layer. Situations where salt is locally cropping out at the seabed are consistent with clastic sediments flanking laterally the structures which are involved in progressive unconformity and differential compaction processes, and are covered by a cap rock at the top (Fig. 16). The partial accounting of the evaporite layer for each structure is compatible with the deformation history. A larger initial volume of salt in the proximal part of the section migrates progressively towards the structural high in the section center, pushing massive clastic material to more distal portions. The difference of salt material between the two sections results in a different structural restoration for each one. The salt laterally flowing out in each section is not proportional to the salt existing at present day in the section. It increases from 75 % in the A-A' section to 160 % in the B-B' section. Whereas the amount of salt is 2.4 times greater at the present day in the A-A' section than in the B-B' section, this relationship is only 1.6 times for the Aptian restored outcome, at the initial deformation stage of salt sequence. These variations suggest that the distribution of salt was spatially more homogeneously in the past and the salt layer was more efficiently pushed away in the B-B' section. The restoration solution considered no synchronism between the extension processes in the salt gravity-driven deformation domain and those deforming the layers below the salt. The accumulated extension represents an increase of almost 60% for the section in the package deformed by salt tectonics in the study area. The accumulated extension for the brittle pre-salt domain represents an increase of only approximately 6%. The deformation kinematics is different below and above the ductile salt layer in the study area. They were independent. The salt layer worked as a full detachment. The gravity-driven deformation above this rheological limit showed a more stretched total extension. The results for the brittle deformation domain below this limit are consistent with the assumption of Moreira et al. (2007). For these authors, the master faults of the rift phase ceased their activities or suffered rare reactivations after the deposition of Barra Velha Formation (Fig. 2) and this deformation, almost totally produced before the salt deposition, was fully restored during the restoration cycles of the rifting phase.

4.9. Geohistory based on 1D modelling

Gravitational mass gliding is not usually considered in basin modelling studies, which rather focus on thermal or subsidence aspects. Subsidence history graphs based on wells or pseudo-wells allow simple and useful evolutionary analysis where some implications and consequences of a large horizontal gravitational mass movement for the petroleum

systems could be observed. In many previous 1D studies, phenomena related to salt deformation were solved by the simple salt thickness variation (diapirism). The restoration results to the spatial deformation of the structures through time gave new dimensions for 1D modelling studies, with new approaches for time and space. The points of a fictive vertical line composing a pseudo-well in the section at present day came from upstream positions in the former restoration outcomes, due to a differential motion controlled by the cumulative amounts of extension through time. On the other hand, a fictive vertical window in the same section position shows how the overburden that glides to downstream situations is progressively replaced by the former neighboring overburden. For instance, the initial overburden that was deposited above this fictive point in Albian times has been moved away, being now replaced by another segment of the overburden which was deposited farther west, due to the ongoing gravitational gliding. These approaches can be differentially applied to calibrate thermal models based, for example, on vitrinite reflectance data from younger layers and to analyze the evolution of a source rock deposited below the salt layer. Built from restored sections results, the subsidence and overburden historical graphs here presented (Fig. 17) replace the traditional image of layers under increasing compaction by layers under tectonic movement. The relevance of the results on thermal effects that can be analyzed with this approach depends on the magnitude of the accumulated lateral movement that the system has undergone. As most of the thermal data are obtained in more recent layers and their lateral shifting due to the gravitational gliding is not so large, no great differences are observed compared to a traditional approach. However, for thermal data obtained in a stretched layer that was moved kilometers away, the difference may be significant as, for example, when the layer is moved from a diapir flank to an overburden position of a source rock kitchen. These graphs include not only the lateral motion of bodies resulting from gravitational gliding by halokinesis but also illustrate a reference evolutionary scenario to constraint various parameters such as bathymetry and isostasy. Even if a bathymetry history was designed as a coherent evolutionary model, some imperfections can be observed through time in a few restoration outcomes, resulting from handcraft restorations of the modules targeting low-resolution bathymetric data. Without any control for the restoration of the older units, a dry depression is postulated to the pre-salt sequence, prior to the deposition of a thick salt layer, especially when the salt isostatic response is too small to prevent the creation of a positive relief of salt above sea level. Following this transitional isostatic jump provided by salt deposition, a shallow marine deposition took place during the Albian and gradually changed to a scenario of maximum water depth observed at the Turonian. This trend toward restoration cycles involving even deeper waters is reversed by a progradational clastic sedimentation in the Late Cretaceous.

Since then and until the present day, an evolutionary change accounted for the progressive building of the current basin configuration, during a period characterized by slower salt tectonics. The initial restored salt layer is very thick in all graphs. It allows smoothed bathymetry adjustments to all isostatic calculations, considering the salt layer as a compensating element. The major adjustment problems seem to stand out at the transition between the five evolutionary

sequences described before. Even if there is uncertainty about the initial thickness of salt, the restored salt volume in the results seems to be excessive. Assuming a large availability of salt, these 1D graphs suggest that most of the accommodation space created during the salt tectonics is due to the lateral expulsion of salt under the continuous burial of the Santos Basin, providing a good summary of the progradation history (Fig. 17). Pseudo-well 1B shows significant proximal sedimentation easily accommodated in Albian to Cenomanian times; whereas pseudo-well 2A shows Late Cretaceous progradation and pseudo-well 4A shows Cenozoic representative thickness. The clastic progradation from Late Cretaceous imposes greater deformation on the salt layer. Pseudo-wells 1B, 2A and 4A in Figure 17 are positioned in post-salt depocenters (salt windows), from where thick salt layers had been gradually squeezed at different times (Turonian for pseudo-well 1B, top Cretaceous for pseudo-well 2A and Miocene for pseudo-well 4A). In contrast, pseudo-well 3B is positioned above a thick salt wall close to the Cabo Frio Fault. This pseudo-well shows the Late Cretaceous evolution of a minibasin, coeval with a progradation event. It also shows that the salt layer underwent a relatively continuous thickening during its lateral gliding away from more proximal areas. Major problems found in these graphs are linked to periods with the higher sedimentation rates: the more intense is the deformation under higher clastic supply, the greater are the difficulties to set bathymetry and isostasy for the restored timing. These graphs represent a good quality control for the restoration process itself. Because the entire restoration process has some intervention from the interpreter, several deviations could be unintentionally introduced in the meantime. The simultaneous visualisation of these 1D graphs can be a useful tool to identify the critical points and to get better results.

5. Conclusions

The approach integrating structural restoration tools with isostatic control and paleo bathymetric model is very important to the obtained results. The configuration of the transition from rifting to drifting phases is a consequence of the salt tectonics backward restoration. Apparently, the results help to characterize the general complex framework for the geometry of the salt depositional environment, but they are not conclusive to provide insights about the pre-existing rifting depositional domains and facies. For the post-salt sequences, deformed by halokinesis, the brittle clastic package developed early in the proximal domains in contrast with the thin sequences of the distal portions, shaped by ductile rheology of the thick salt layer. In the latter domain, these thin sequences either behave as small rafts during early extension or develop a subsequent and continuous compression in the minibasins area.

A conservative salt volume is not a realistic constraint in the study area. A first approximation was provided by the 2D nature of the restoration while salt movements occur in a complex 3D world. In addition, the extrapolated salt brought from distal areas, coherent with regional knowledge, allows a more realistic restoration scenario for both A-A' and B-B'

geological sections. This approach allowed a decoupled restoration where bathymetry controls the sequence above the salt, isostasy controls the package below the salt and the ductile salt layer works as an element of local compensation.

1
2 Paleo-bathymetry data and flexural isostasy calculations provide guidelines to restore independent packages above and
3
4 below the ductile salt layer. Simplified and arbitrary parameters assumed in the restoration processes did not detract from
5
6 the methodology approach. Recognized problems were produced by handmade interventions during the simple shear
7
8 and flexural slip operations and also by the lack of isostatic compensation of the lateral movement of the restored
9
10 modules.

11
12 Geohistory 1D analysis established from 2D section restoration results are complementary tools to improve the whole 2D
13
14 palinspastic process. Inconsistencies produced during restoration steps can be easily observed in these graphs and use
15
16 again as a new input for further optimization loops. They allow a consistent evaluation of the local bathymetry variation
17
18 through time. The 1D subsidence graphs confirm that the sedimentary evolution in the study area results from a continuous
19
20 sedimentary progradation. They illustrate salt welding first in proximal portions and, consequently, salt windows gradually
21
22 opening over time from these regions to the most distal ones. They also provide a different approach based on the lateral
23
24 mass movement for 1D thermal modelling.

25
26 The simplified 2D restoration approach with independent and interactive bathymetry, isostasy and modules
27
28 operation controls here presented could provide easy guidelines for new 3D restoration solutions and
29
30 developments.

31
32
33
34
35
36
37
38
39
40
41
42
43
44
45
46
47
48
49
50
51
52
53
54
55
56
57
58
59
60
61
62
63
64
65

Acknowledgments

1
2First of all, we would like to thank Petrobras for all support during the present research. We also express our
3
4gratitude to Sylvia Anjos, François Roure, Henrique Penteado, Luiz Antonio Freitas and Cláudia Lima who
5
6made important contributions to this paper. Our thanks to all the Petrobras E&P petroleum systems geologists,
8
9the IFP Energies Nouvelles researchers and the Tecgraf IT support team. This paper would not have been
10
11finalized without their support, comments and suggestions during the entire restoration job.
12

13
14
15
16
17
18
19
20
21
22
23
24
25
26
27
28
29
30
31
32
33
34
35
36
37
38
39
40
41
42
43
44
45
46
47
48
49
50
51
52
53
54
55
56
57
58
59
60
61
62
63
64
65

References

- 1
2Almeida, F.F.M., 1976. The system of continental rift bordering the Santos Basin, Brazil. *Anais Academia Brasileira*
3
4*Ciencias*, 48 (suppl.), 15-26.
- 5
6Assine, M.L., Correa, F.S., Chang, H.K., 2008. Migration depocenters in the Santos Basin: importance for hydrocarbon
7
8exploration (Migração de depocentros na Bacia de Santos: importância na exploração de hidrocarbonetos). *Revista*
9
10*Brasileira de Geociências* 28, (2) supplement, 111-127.
- 11
12Arai M., 1988. Geochemical reconnaissance of the Mid-Cretaceous anoxic event in the Santos Basin, Brazil. *Revista*
13
14*Brasileira de Geociências* 18, 273-282.
- 15
16Bender, A.A., Mello, U.T., Chang, H.K., 1989. Bidimensional reconstitution of the geologic history of sedimentary basins:
17
18theory and its application in the Campos Basin (Reconstituição bidimensional da história geológica de bacias
19
20sedimentares: teoria e uma aplicação na bacia de Campos). *Boletim de Geociências da Petrobras* 3 (1/2), 67-85.
- 21
22Braga, L.F.S., Costa, C.M., Gama, F., Fontoura, C., Cunha, A.S., Dourado, F., Correa, F.S., 2003. Magneto-Structural
23
24Imaging (MSI) and Regional Basement of the Santos Basin, Brazil. *International Congress of The Brazilian Geophysical*
25
26*Society*, 8, Rio de Janeiro, SBGf. CD-ROM. 4 p.
- 27
28Cande, S.C., Rabinowitz, P.D., 1978. Mesozoic seafloor spreading bordering conjugate continental margins of Angola
29
30and Brazil. *Proceedings of Offshore Technology Conference*, Houston, Texas, OTC3268, pp. 1869-1871.
- 31
32Carminatti, M., Wolff, B., Gamboa, L.A.P., 2008. New exploratory frontiers in Brazil. 19th World Petroleum Congress,
33
34Madrid, Spain, WPC proceedings.
- 35
36Cobbold, P.R., Szatmari, P., 1991. Radial gravitational gliding on passive margins. *Tectonophysics* 188, 249-289.
- 37
38Cobbold, P.R., Meisling, K.E., Mount, V.S., 2001. Reactivation of an obliquely rifted margin, Campos and Santos Basin,
39
40Southeastern Brazil. *Am. Assoc. Petrol. Geol. Bull.* 85, (11), 1925-1944.
- 41
42Davison, I., 2007. Geology and tectonics of the South Atlantic Brazilian salt basins, in: Ries, A.C., Butler, R.W.H.,
43
44Graham, R.H. (Eds.), *Deformation of the continental crust: The legacy of Mike Coward*. Geological Society, London,
45
46Special Publications, 272, 345-359.
- 47
48Demercian, L.S., 1996. Halokinesis in evolution of the south of Santos Basin from the Aptian to Upper Cretaceous (A
49
50halocinese na evolução do sul da Bacia de Santos do Aptiano ao Cretáceo superior). Master Dissertation, Universidade
51
52Federal do Rio Grande do Sul, Brazil.
- 53
54Dias, J.L., 1998. Stratigraphic and sedimentological analysis of Aptian stage in part of the eastern margin of Brazil and
55
56Malvinas Plateau – Considerations about the first marine incursions and ingressions of the South Atlantic Ocean (Análise
57
58sedimentológica e estratigráfica do andar aptiano em parte da margem leste do Brasil e no Platô das Malvinas -
59
60
61
62
63
64
65

considerações sobre as primeiras incursões e ingressões marinhas do oceano atlântico sul meridional). PhD thesis,

Universidade Federal do Rio Grande do Sul, Brazil.

- 1
2 Freitas, J.T.R., 2006. Evaporite depositional cycles of the Santos Basin: an analysis of cyclostratigraphy data from two
3
4 wells and seismic traces (Ciclos deposicionais evaporíticos da Bacia de Santos: uma análise cicloestratigráfica a partir de
5
6 dados de 2 poços e de traços de sísmica). Ph.D thesis, Universidade Federal do Rio Grande do Sul, Porto Alegre, Brazil.
7
8 Gamboa, L.A.P., Machado, M.A.P., Silveira, D.P., Freitas, J.T.R., Silva, S.R.P., 2008. Evaporites stratigraphy in the South
9
10 Atlantic: interpretation of seismic and tectonic-stratigraphic control in the Santos Basin (Evaporitos estratigráficos no
11
12 atlântico sul: interpretação sísmica e controle tectono-estratigráfico na bacia de Santos), in Mohriak, W.U., Szatmari, P.,
13
14 Anjos, S.M.C. (Eds.), Salt: geology and tectonics. Examples from Brazilian basins (Sal: geologia e tectônica. Exemplos
15
16 nas bacias brasileiras), pp. 340-360.
17
18 Garcia, S.F.M., 1999. Three-dimensional study of effects of halokinesis in passive margins (Estudo tridimensional de
19
20 efeitos da halocinese em margens passivas). Master Dissertation, Universidade Federal de Ouro Preto, Brazil.
21
22 Gomes, P.O., Kilsdonk, B., Minken, J., Grow, T., Barragan, R., 2009. The Outer High of the Santos Basin, southern São
23
24 Paulo Plateau, Brazil: pre-salt exploration outbreak, paleogeographic setting, and evolution of the syn-rift structures.
25
26 Search and Discovery Article #10193 (<http://www.searchanddiscovery.net/documents/2009/10193gomes/index.htm>).
27
28 Gomes, P.O., Parry, J., Martins, W., 2002. The Outer High of the Santos Basin, southern São Paulo Plateau, Brazil:
29
30 Tectonic. Am. Assoc. Petrol. Geol. Hedberg Conference, Hydrocarbon habitat of volcanic rifted passive margins,
31
32 Stavanger, Norway, 8-11.
33
34 Gradstein, F.M., Ogg, J.G., Smith, A.G., 2004. A geologic time scale 2004. Cambridge University Press.
35
36 Gross, G.M., 1972. Oceanography: a view of the Earth. Prentice-Hall, Inc., Englewood, New Jersey.
37
38 Guerra, M.C.M., 2008. Role of halokinesis in controlling structural styles and sediment dispersal pattern in the Santos
39
40 Basin, offshore SE Brazil. PhD thesis, University of Edinburgh, UK, 270.
41
42 Guimarães, P.P., Almeida, H.P., Kowsman, R.O., Costa, M.P. and Boa Hora, M.P., 1982. Gravimetric modelling in São
43
44 Paulo Plateau southern portion and its geological implications (Modelagem gravimétrica na porção sul do Platô de São
45
46 Paulo e suas implicações geológicas). XXXII Brazilian Geological Congress, Salvador, Bahia, 4, 1570 - 1575.
47
48 Henry, S., Brumbaugh, W.D., Cameron, N.R., 1995. Presalt source rock development on Brazil's conjugate margin: West
49
50 African examples. 1st Latin American Geophysical Conference, Rio de Janeiro, August, extended abstract, pp.3.
51
52 Hudec, M.R., Jackson, M.P.A., Schultz-Ela, D.D., 2009. The paradox of minibasin subsidence into salt: clues to the
53
54 evolution of crustal basins. Geol. Soc. Am. Bull. 121, 201-221.
55
56 Jan, N., Jackson, M.P.A., Hudec, R., 2009. Tectonics of passive margin salt basins: crustal structure of the Gulf of Mexico
57
58 and South Atlantic during salt deposition. Am. Assoc. Petrol. Geol., Annual Convention and Exhibition, Denver, Colorado,
59
60 Abstract.
61

Jackson, M.P.A., Cramez, C., Fonck, J.M., 2000. Role of subaerial volcanic rocks and mantle plumes in creation of South Atlantic margins: implications for salt tectonics and source rocks. *Marine and Petroleum Geology*, 17, 477-498.

1
2 Karner, G.D., 1982. Spectral representation of isostatic models. *BMR Journal of Australian Geology*, 7, 55-62.
3

4 Karner, G.D., Driscoll, N.W., Barker, D.H.N., 2003. Syn-rift regional subsidence across the West African continental
5
6 margin: the role of lower plate ductile extension, in: Arthur, T.J., MacGregor, D.S., Cameron, N.R. (Eds.), *Petroleum
7
8 Geology of Africa: New themes and developing technologies*. Geological Society, London, Special Publications, 207,
9
10 105–129.
11

12 Karner, G.D., Gamboa, L.P.A., 2007. Timing and origin of the South Atlantic pre-salt sag basins and their capping
13
14 evaporites, in: Schreiber, B., Lugli, S., Babel, M., *Evaporites through space and time*. Geological Society Special
15
16 Publication, 285, 15-35.
17

18 Kumar, N., Gamboa, L.A.P., Scheiber, B.C., Mascle, J., 1977. Geologic history and origin of São Paulo Plateau
19
20 (southeastern Brazilian margin), comparison with the Angolan margin, and early evolution of the northern South Atlantic.
21
22 Initial reports of the Deep Sea Drilling Project. Washington. D.C. 39, 927-945.
23

24 Lavier, L.L., Manatshal, G., 2006. A mechanism to thin the continental lithosphere at magma-poor margins. *Nature*, 440,
25
26 324–328.
27

28 Lerche, I., Petersen, K., 1995. *Salt and sediments dynamics*, CRC Press.
29

30 Marton, L.G., Tari, G.C., Lehmann, C.T., 2000. Evolution of the Angolan passive margin, West Africa, with emphasis on
31
32 post-salt structural styles, in: Mohriak, W.U., Talwani, M. (Eds.), *Atlantic rifts and continental margins*. American
33
34 Geophysical Union Geophysical monography, 115, 129-149.
35

36 Mascle, J.R., Renard, V., 1976. The marginal Sao Paulo Plateau, comparison with the southern Angolan margin.
37
38 *Brazilian Academy of Sciences*, 48, 179-190.
39

40 McKenzie, D.P., 1978. Some remarks on the development of sedimentary basins. *Earth Planet. Sci. Letters*, 40, 25–32.
41

42 Meisling, K.E., Cobbold, P.R., and Mount, V.S., 2001. Segmentation of an obliquely rifted margin, Campos and Santos
43
44 basins, southeastern Brazil. *Am. Assoc. Petrol. Geol. Bull.* 85, 1903-1924.
45

46 Mohriak, W.U., 2001. Salt tectonics, volcanic centers, fracture zones and their relationship with the origin and evolution of
47
48 the South Atlantic Ocean: geophysical evidence in the Brazilian and West African margins, in: SBGf, International
49
50 Congress of The Brazilian Geophysical Society, 7, Salvador–Bahia – Brazil, Expanded Abstract, pp. 1594.
51

52 Mohriak, W.U., Szatmari, P., 2001. Salt tectonics and sedimentation along Atlantic margins: insights from seismic
53
54 interpretation and physical models. *Geol. Soc. America, Memoir* 193, 131-151.
55

56 Moreira, J.P.; Madeira, C.V., Gil, J.A., Machado, M.A.P., 2007. Santos Basin (bacia de Santos), in *Stratigraphic charts
57
58 (Cartas estratigráficas)*. *Boletim de Geociências da Petrobras*, 15, (2), 531-549.
59
60
61
62
63
64
65

Pereira, M.J., Barbosa, C.M., Agra, J., Gomes, J.B., Aranha, L.G.F., Saito, M., Ramos, M.A., Carvalho, M.D., Stamato, M., Bagni, O., 1986. Stratigraphy of the Santos Basin: sequences analysis, depositional systems and litho-stratigraphic revision (Estratigrafia da Bacia de Santos: Análise das sequências, sistemas deposicionais e revisão lito-estratigráfica). XXXIV Brazilian Geological Congress, (1), 65-79.

Pereira M.J., Macedo J.M., 1990. Santos Basin: perspectives of a new petroleum province in the Southeastern Brazilian continental platform (A Bacia de Santos: perspectivas de uma nova província petrolífera na plataforma continental sudeste brasileira). Boletim Geociências da Petrobrás, 4, 3-11.

Pereira, M.J., Feijó, F.J., 1994. Santos Basin (Bacia de Santos). Boletim de Geociências da Petrobras, Rio de Janeiro, 8, (1), 219-234.

Pinet, P.R., 1996. Invitation to oceanography. St. Paul, MN, West Publishing Company, ISBN 0-314-06339-0.

Roberts, A.M., Kuszniir, N.J., Yielding, G., Styles, P., 1998. 2D flexural backstripping of extensional basins: the need for a sideways glance. Petroleum Geoscience, 4, 327–338.

Rouby, D., Cobbold, P.R., Szatmari, P., Demercian, S., Coelho, D., Rici, J.A., 1993. Least-squares Palinspastic Restoration of Regions of Normal Faulting – Application to the Campos Basin (Brazil). Tectonophysics, 221, 439-452.

Rowan, M.G., 1993. A systematic technique for the sequential restoration of salt structures. Tectonophysics, 228, 331-348.

Scotchman, I.C., Marais-Gilchrist G., Souza, F.G., Chaves, F.F., Atterton, L.A., Roberts, A., Kuszniir, N.J., 2006. A failed sea-floor spreading centre, Santos Basin, Brasil. Rio Oil & Gas Conference. IBP. Rio de Janeiro, Abstract.

Szatmari, P., Demercian, L.S., 1993. Salt Tectonics in the southern Brazilian margin (Tectônica de sal na margem sudeste brasileira). SBGf, Congresso Internacional da Sociedade Brasileira de Geofísica, Anais 3, 1347-1351.

Zalán, P.V., Severino, M.C.G., Oliveira, J.A.B., Magnavita, L.P., Mohriak, W.U., Gontijo, R.C., Viana, A.R., Szatmari, P., 2009. Stretching and thinning of the upper lithosphere and continental-oceanic crustal transition in Southeastern Brazil. Am. Assoc. Petrol. Geol., International Conference and Exhibition, Rio de Janeiro, Brazil, Abstract.

Watts, A.B., 1982. Tectonic subsidence, flexure and global changes in sea level. Nature, 297, 469-474.

Williams, B.G. and Hubbard, R.J., 1984. Seismic stratigraphic framework and depositional sequences in the Santos Basin, Brazil. Marine Petrol. Geol., 1, (2), 90-104

Weijermars, R.; Jackson, M.P.A., Vendeville, B.C., 1993. Rheological and tectonic modeling of salt provinces. Tectonophysics 217, 143-174.

Wernicke, B., 1981. Low-angle normal faults in the Basin and Range Province: nappe tectonics in an extending orogen. Nature, 291, 645-648.

Fig. 1 – Regional location map outlining the study area (red polygon) including two restored sections (black lines), six available wells (yellow circles) and four studied pseudo-wells (red circles). Notice the aborted spreading center in the southern region, and its northward propagation along a pre-salt fault trend. Its possible continuity within the study area could account for a local crustal thinning anomaly.

Fig. 2 – Simplified stratigraphic chart of the Santos Basin outlining the fifteen horizons interpreted in the seismic profiles during the study. The major Early Cretaceous progradation event is highlighted between the horizons 03 and 08.

Figure 3 – The two geological sections A-A' and B-B' (see location in Fig. 1) are based on fifteen interpreted horizons. The ten layers above the salt are intensely deformed. The Cabo Frio Fault separates extensional and compressive domains. A proximal low and an intermediate high constitute inherited structures, developed before the onset of salt tectonics. Classical minibasins occur in the distal compressional domain.

Figure 4 – Schematic block diagram of the Santos Basin adapted from the model of Lavier and Manatshal (2006). Notice the aborted southern spreading center where a hypothetical H block can be interpreted. This hypothetical scenario suggests a strongly thinned crustal thickness beneath the São Paulo Plateau.

Figure 5 – The section A-A' is projected on the more regional section A-B-C modified from Carminatti et al. (2008). In the compressional domain, extending eastwards the study area, the evaporites were removed from the more proximal regions and transported towards more distal portions of the margin as mobile blocks, creating accommodation space for the overlying sedimentary pile.

Figure 6 – The shelf break (white points) and foot of the slope (black points) are shown here for the section B-B'. These critical points have been interpreted for each restored horizon above the salt layer, including the Albian carbonates top (H9). Notice the Cabo Frio Fault which limits the thicker proximal domain from the post-salt minibasins that developed in the more distal domain.

Figure 7 – Example of the first restoration steps showing sequential sketches for the partial results of the section A-A'. Notice two desired anchor points of overlying post-salt layers (salt windows), which are highlighted in the step 3, as well as an exaggerated spacing point of the isostasy response to adjustment of the salt layer remarked in the step 4.

Figure 8 – Restoration outcomes of pre-salt stages applied without paleobathymetric data to sections A-A' and B-B'. Notice the extension restored represent less than 10% from the deformed section. The result mountainous terrain reaching up 3,000 meters high in the section A-A' is consistent with the accommodation space needed for the thick salt layer deposition.

Figure 9 – Sections A-A' and B-B' restored at the salt deposition stage. The obtained scenario shows an original salt layer up to 4,000 meters thick in the section A-A'. The faint pink color represents the amount of salt added in order to restore the salt motion towards distal portions.

Figure 10 – Restored profiles of sections A-A' and B-B' for the Albian to Cenomanian stages that shows a climax of the rafting tectonics. The fast extension of the thin Albo-Cenomanian layers is obtained by the underlying salt layer movement, pushed to distal portions by the thick post-salt sediments deposition in the proximal area.

Figure 11 – Restoration model for the Albian carbonates. The seismic image shows the present day configuration of the Albian growth structures. The restoration model requires a formerly thicker salt basin (thicker than 2,500 m) to accommodate the observed thickness growing of the carbonate layers.

Figure 12 – The progradation of the Late Cretaceous restored outcomes for sections A-A' and B-B' showing the development of the Cabo Frio Fault (black arrows) in relationship to the total extension in the study area (red arrows). In association with this differential lateral deformation, the first salt windows were formed in many compartments.

Figure 13 – Restored outcomes of the most recent layers for sections A-A' and B-B'. These sections show that salt tectonics is no longer active in the proximal domain, and remained relatively quiescent within the more distal domain, developing the minibasins.

Figure 14 – First restoration steps showing the decompacted Miocene situation just after the removal of the uppermost layer. The present day in details images is compared with the decompacted scenario of the central image. The decompaction outcome, dependent of the isostatic parameterization, is referred to the present day referential bathymetry (difference in the striped grey area). The detail 1 highlights an isostatic result locally higher than the referential bathymetry (potential erosion) while the detail 2 highlights a relatively lower isostatic position in the minibasins domain (potential aggradation).

Figure 15 – Paleo-bathymetry model through time based on well data for the platform and slope regions (no data available to the continental rise region). The grey area is a superposition of all well data in each area. The red dashed lines are regional bathymetry models for each region. Colored circles (blue, green and red) show the bathymetry expected for each restored age. Notice the pre-existing interpreted depression preceding the deposition of salt.

Figure 16 – Seismic image showing a possible cap rock over the proximal diapirs. Episodes of differential compaction in the post-sal series are observed in the flanks of salt diapirs, surrounding these sub-outcropping structures and delineating local conditions for progressive unconformities.

Figure 17 – Eight graphs based on the restored sections A-A' and B-B' show subsidence and overburden 1D geohistories. The location map provides the pseudo-wells 1B, 2A, 3B and 4A positions. A pseudo-section composed by projected parts shows a continuous progradation from proximal regions to the distal ones from the Albian up to present day.

Figure 1
[Click here to download high resolution image](#)

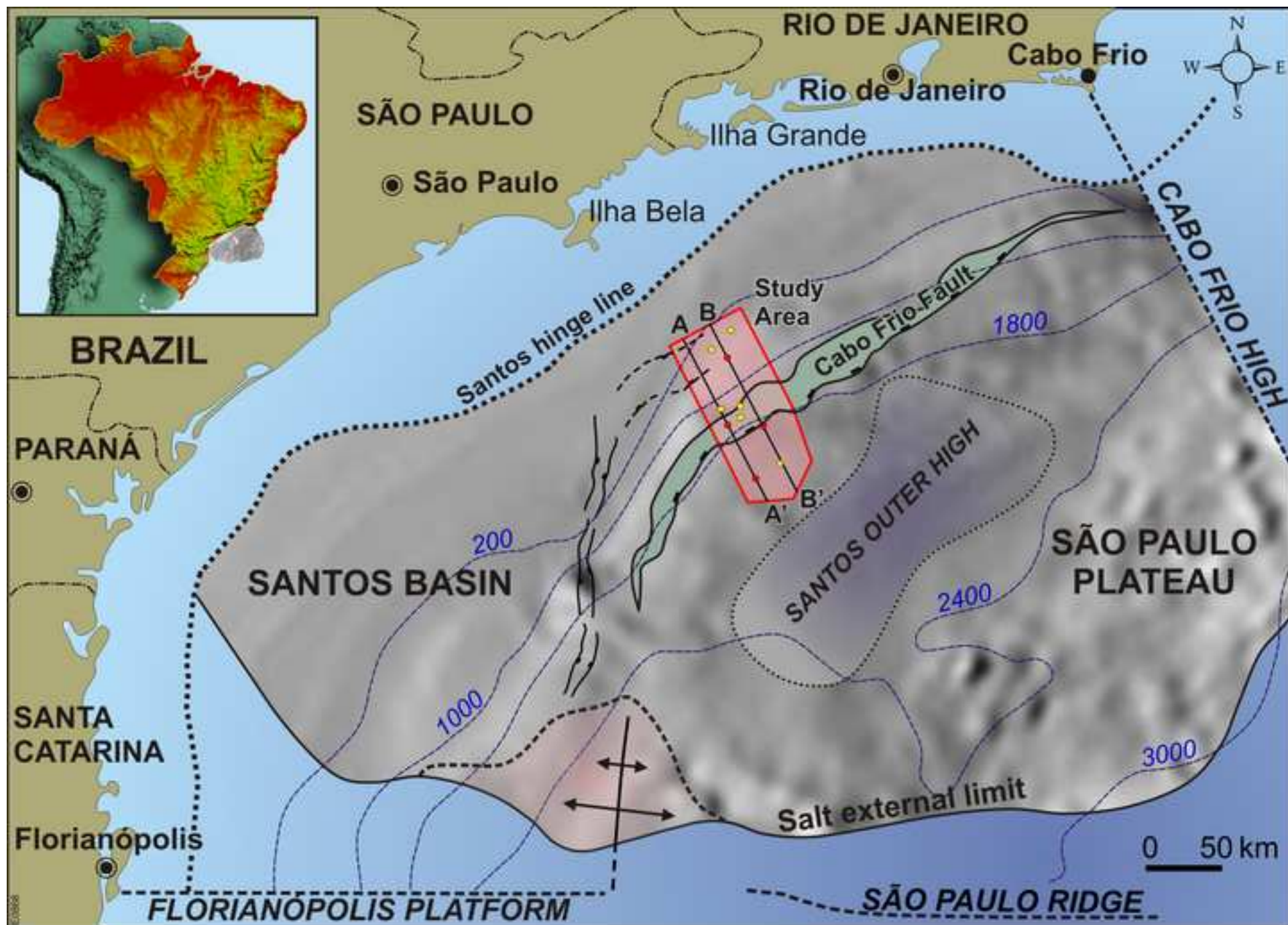


Figure 2
[Click here to download high resolution image](#)

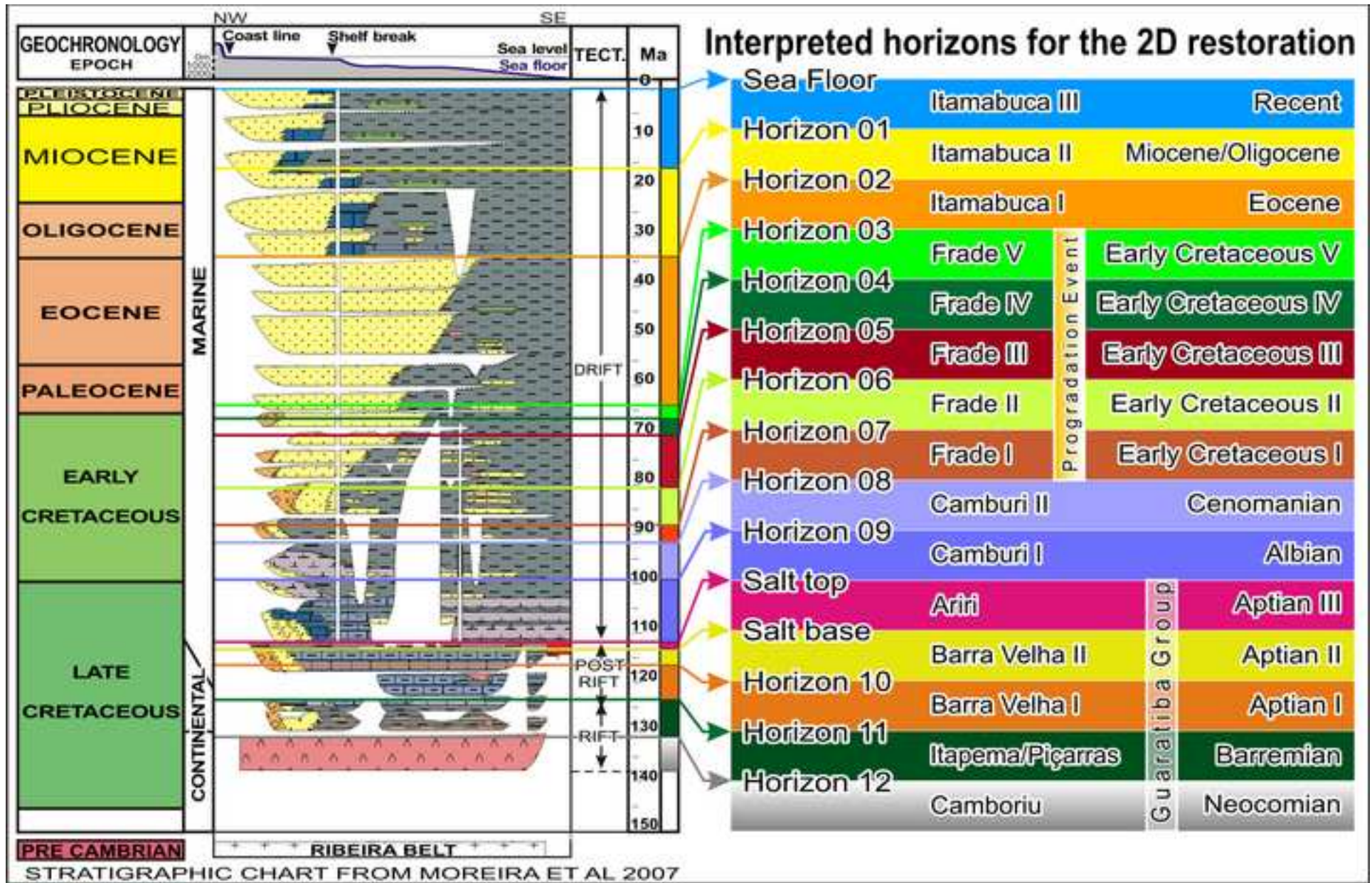


Figure 3
[Click here to download high resolution image](#)

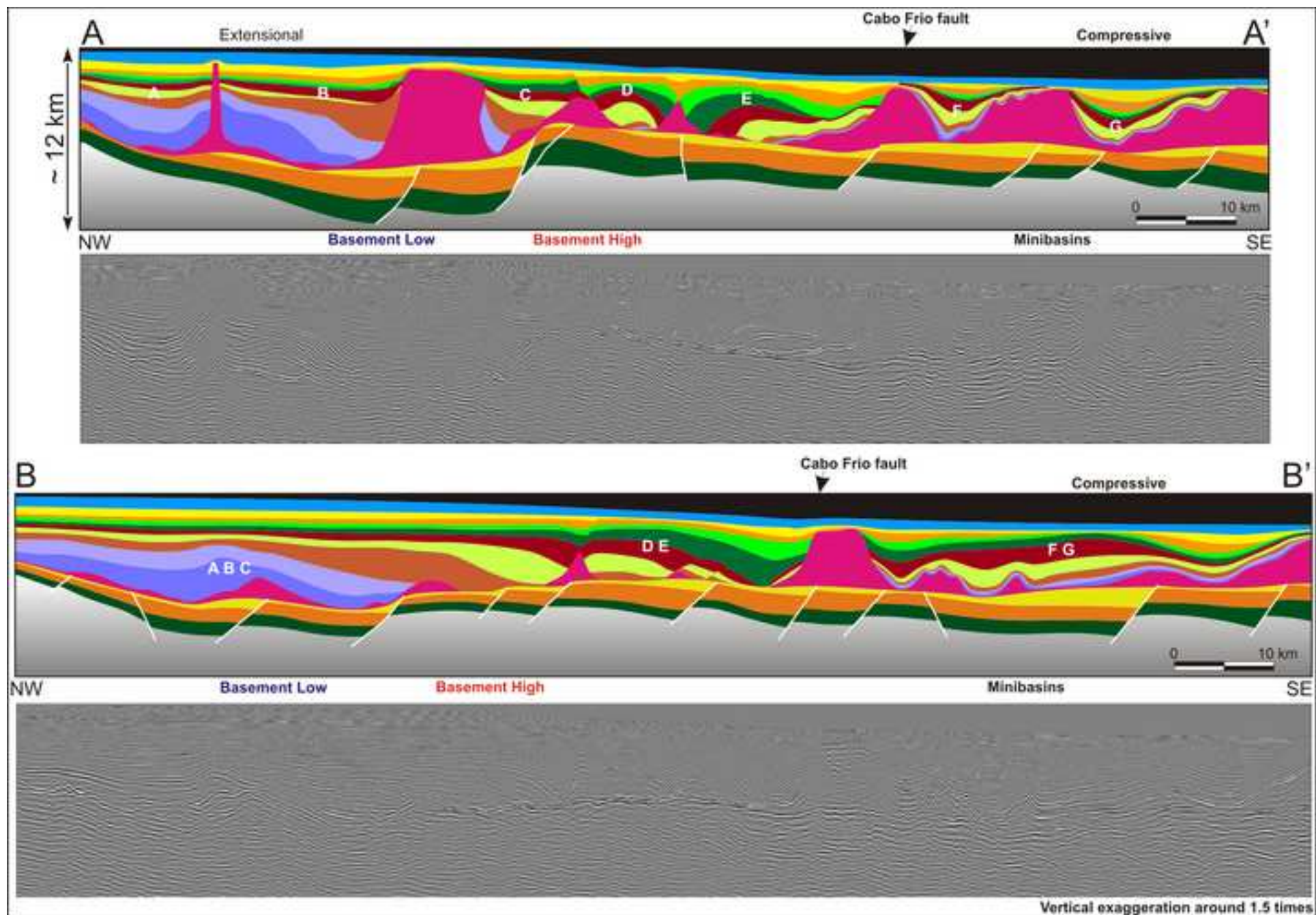


Figure 4
[Click here to download high resolution image](#)

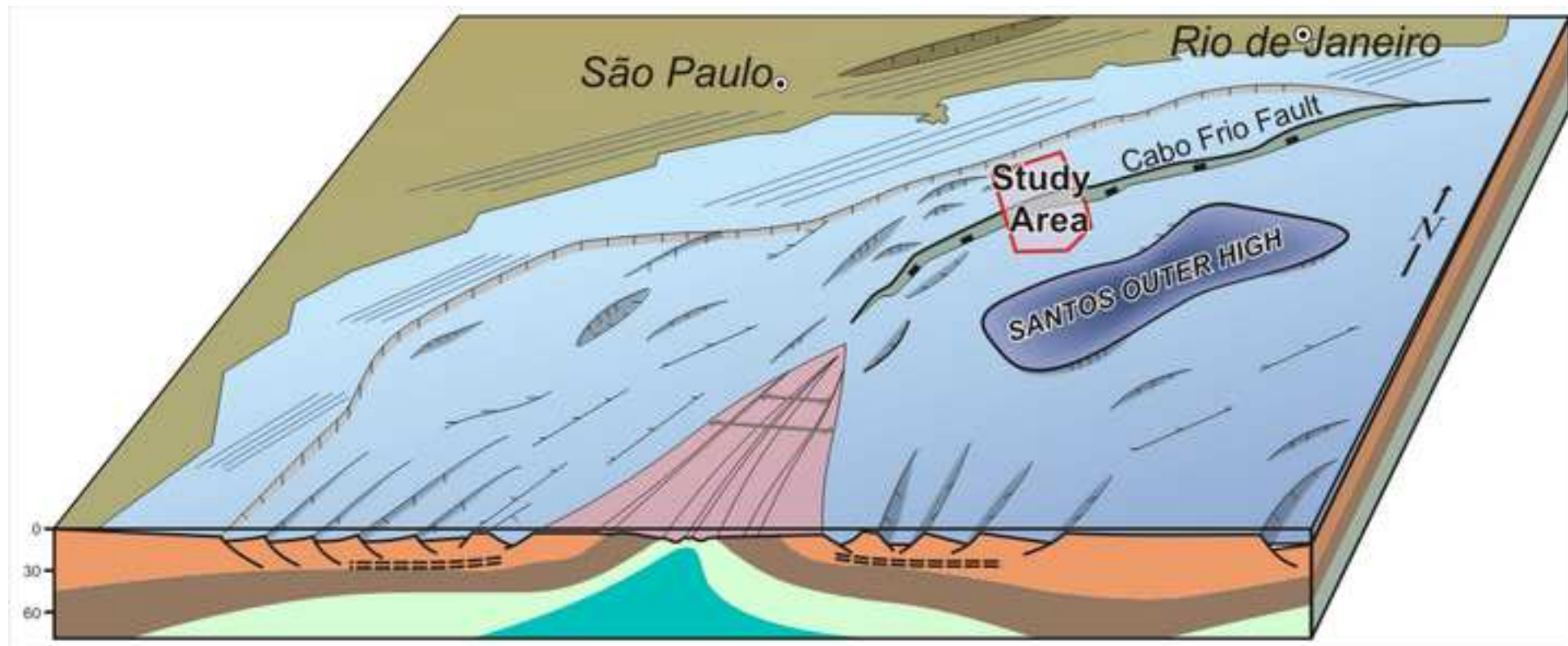


Figure 5
[Click here to download high resolution image](#)

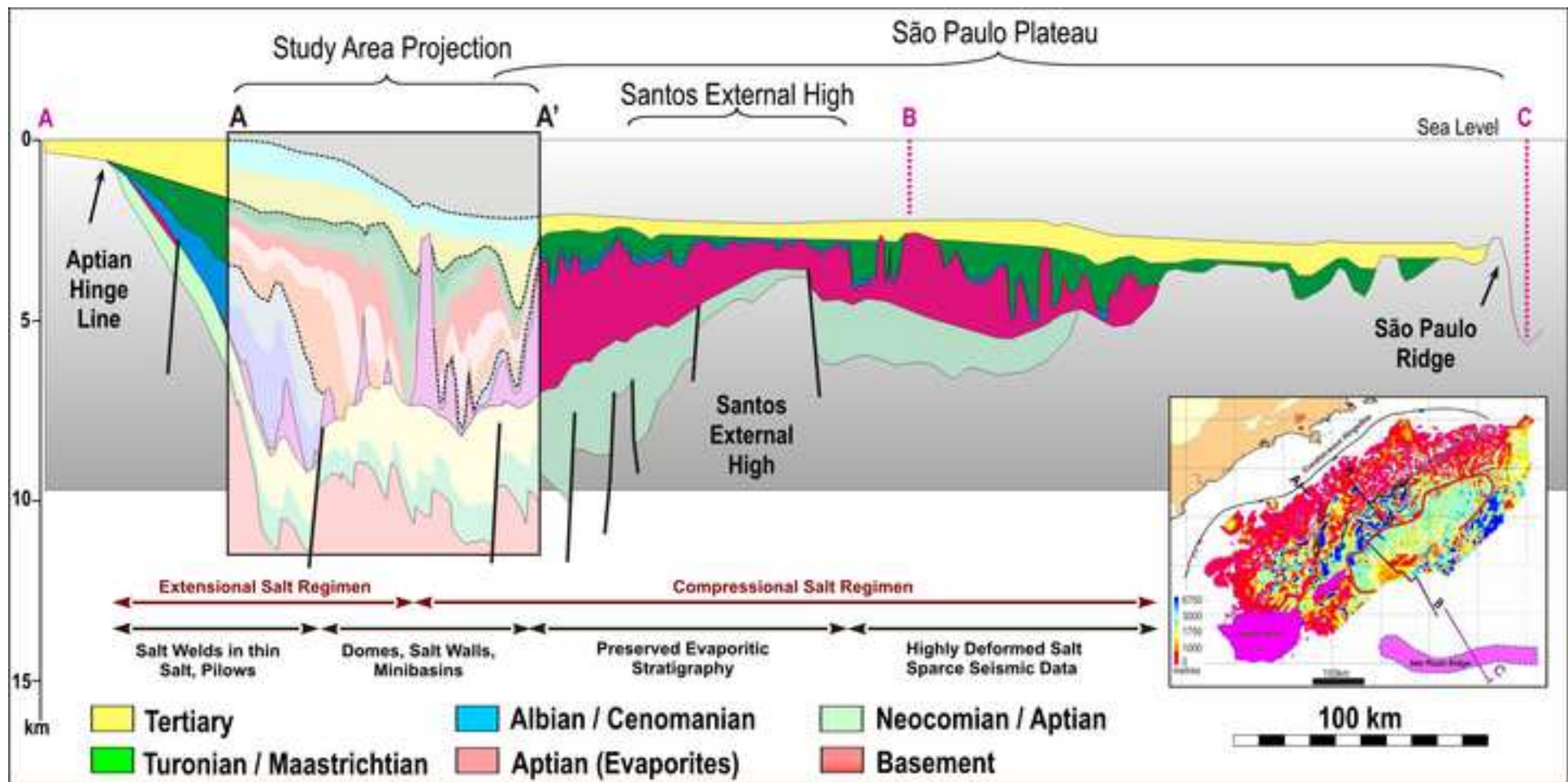


Figure 6
[Click here to download high resolution image](#)

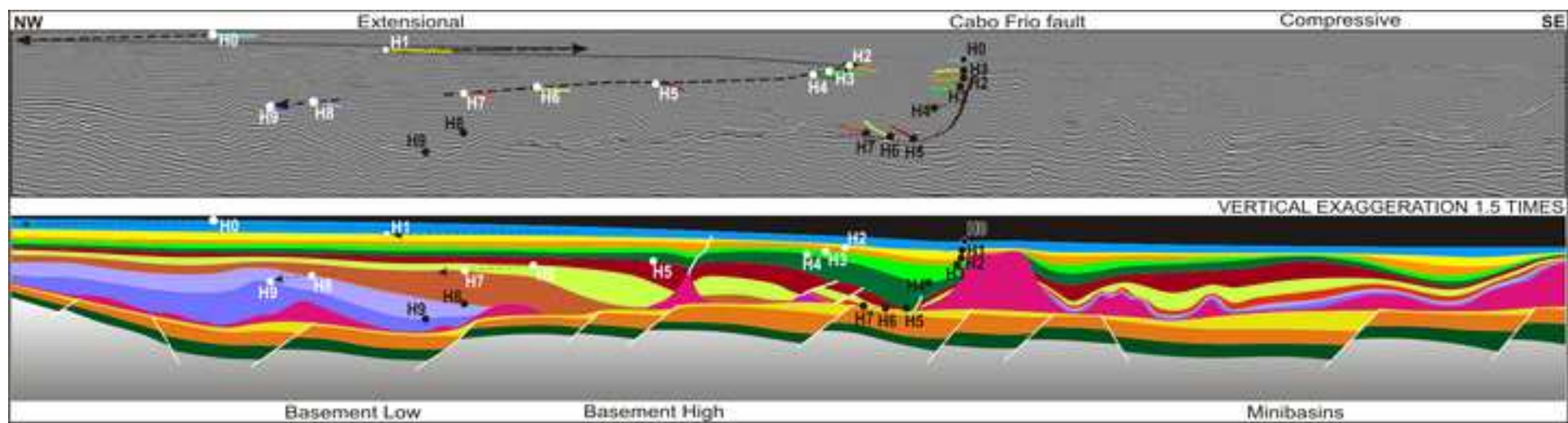


Figure 7
[Click here to download high resolution image](#)

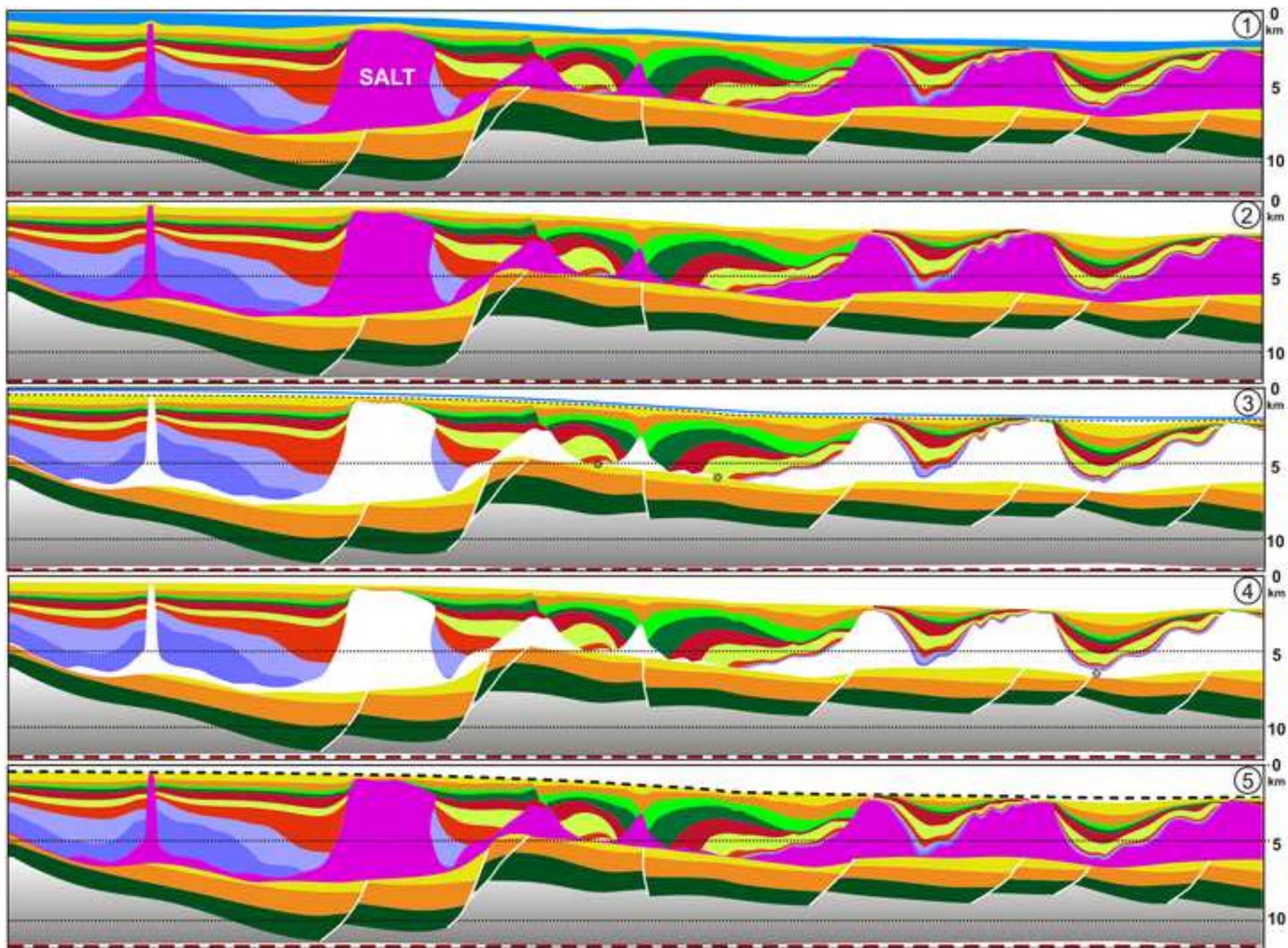


Figure 8
[Click here to download high resolution image](#)

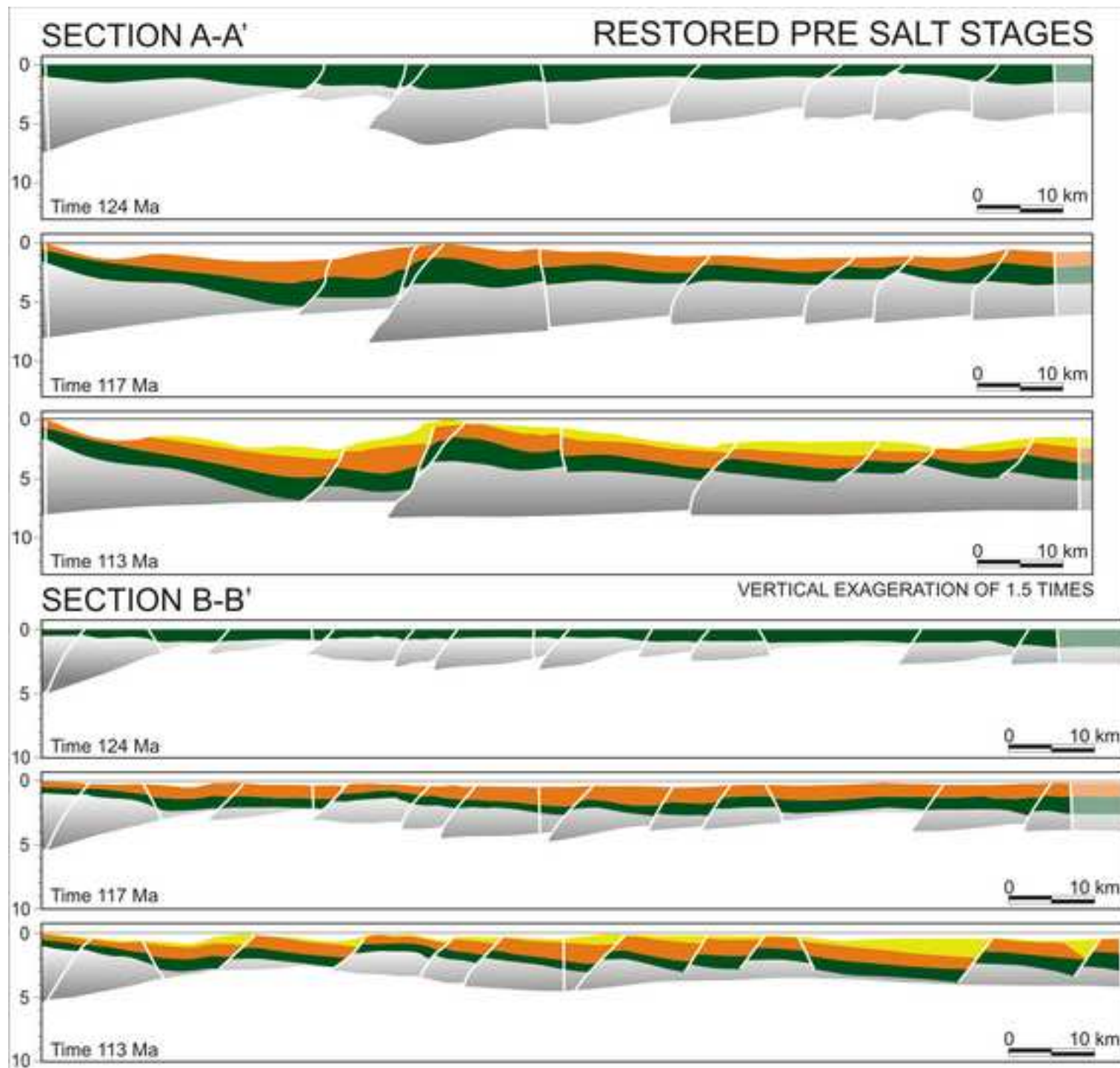


Figure 9
[Click here to download high resolution image](#)

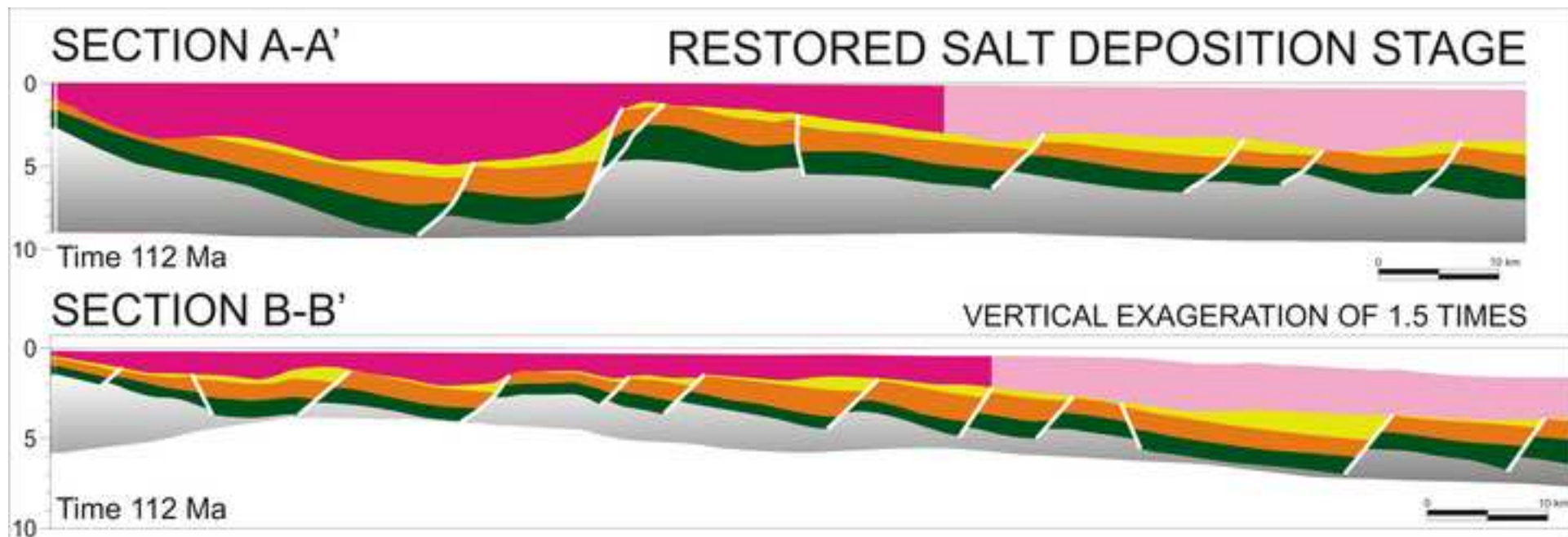


Figure 10
[Click here to download high resolution image](#)

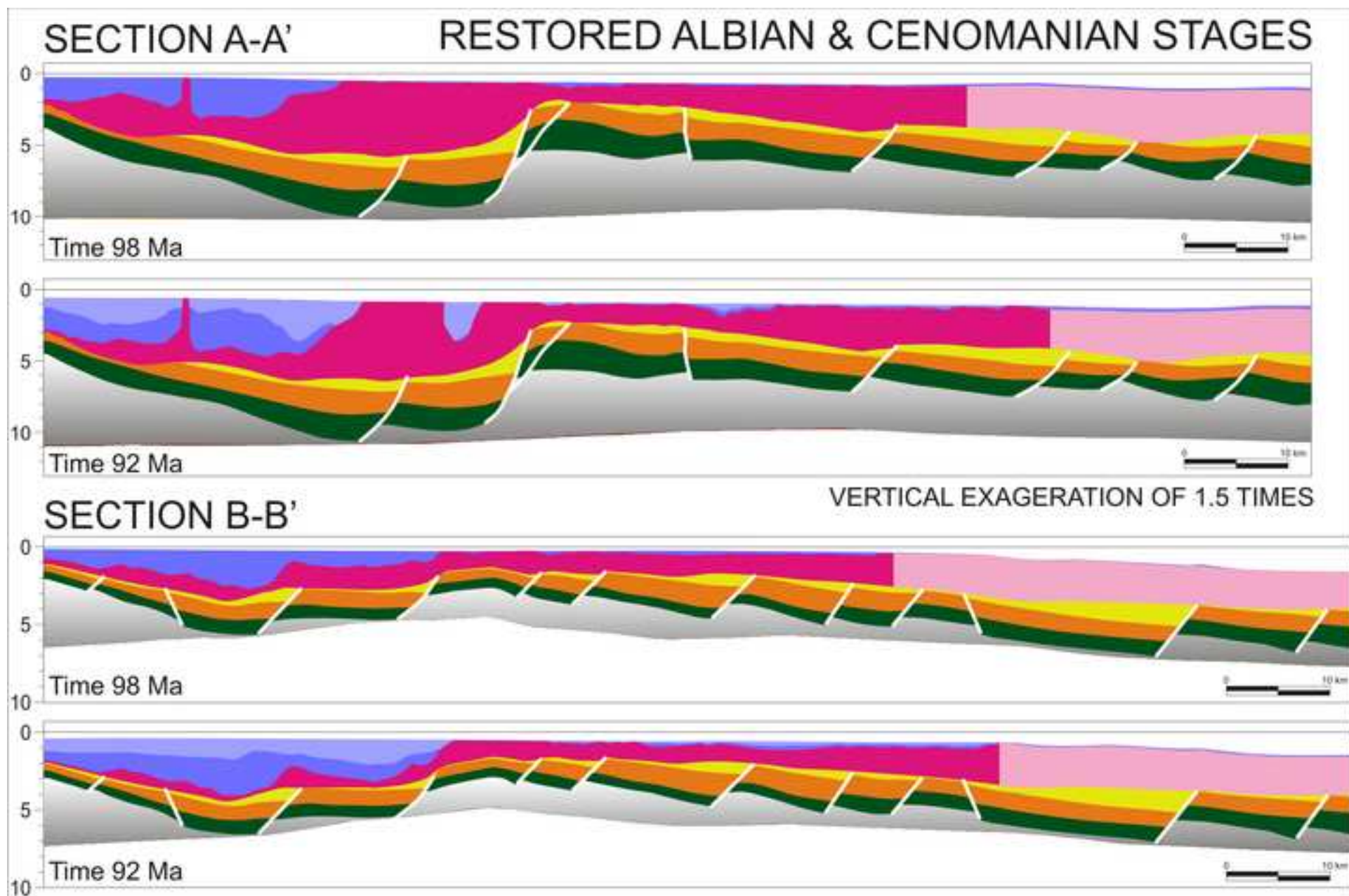


Figure 11
[Click here to download high resolution image](#)

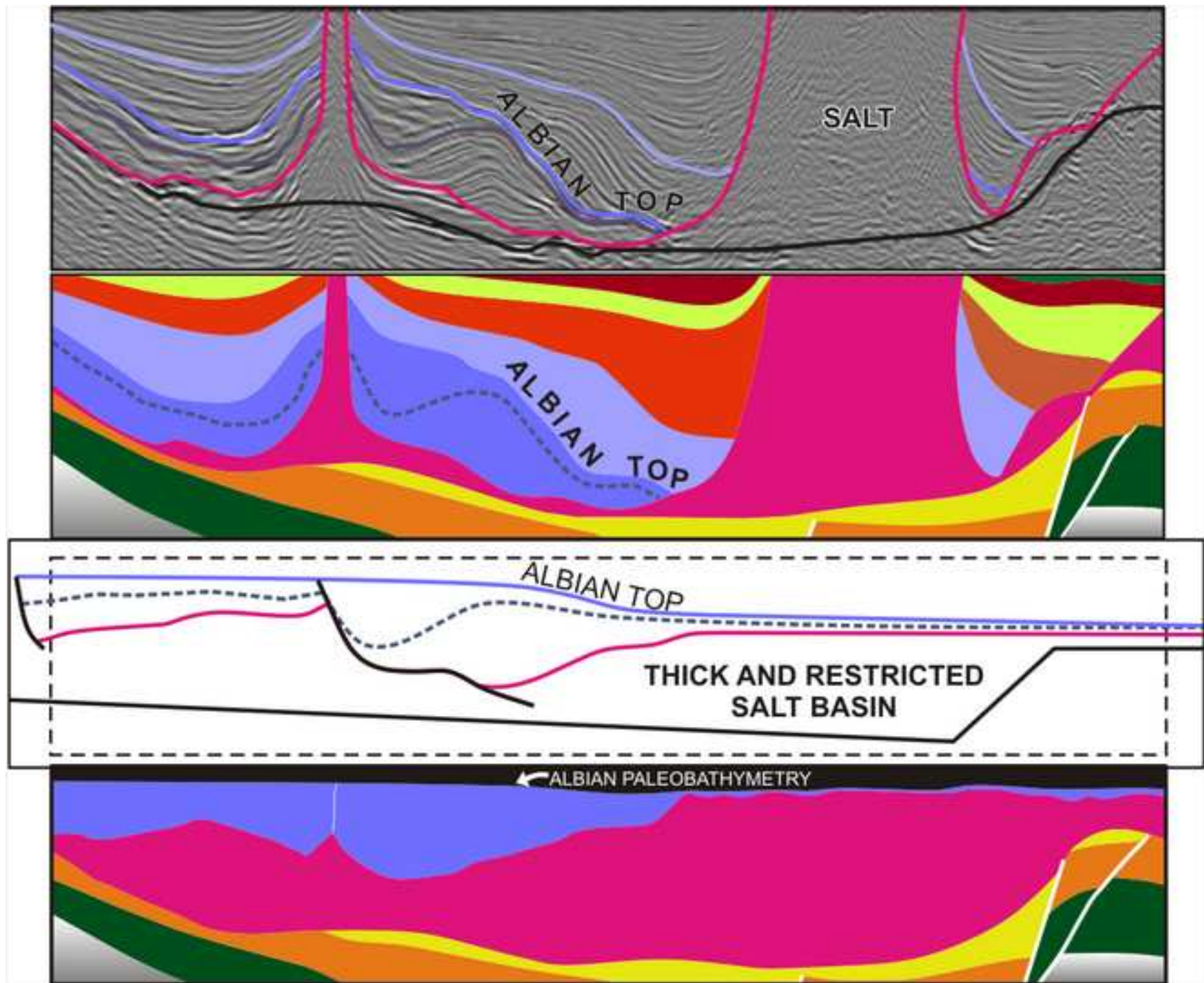


Figure 12

[Click here to download high resolution image](#)

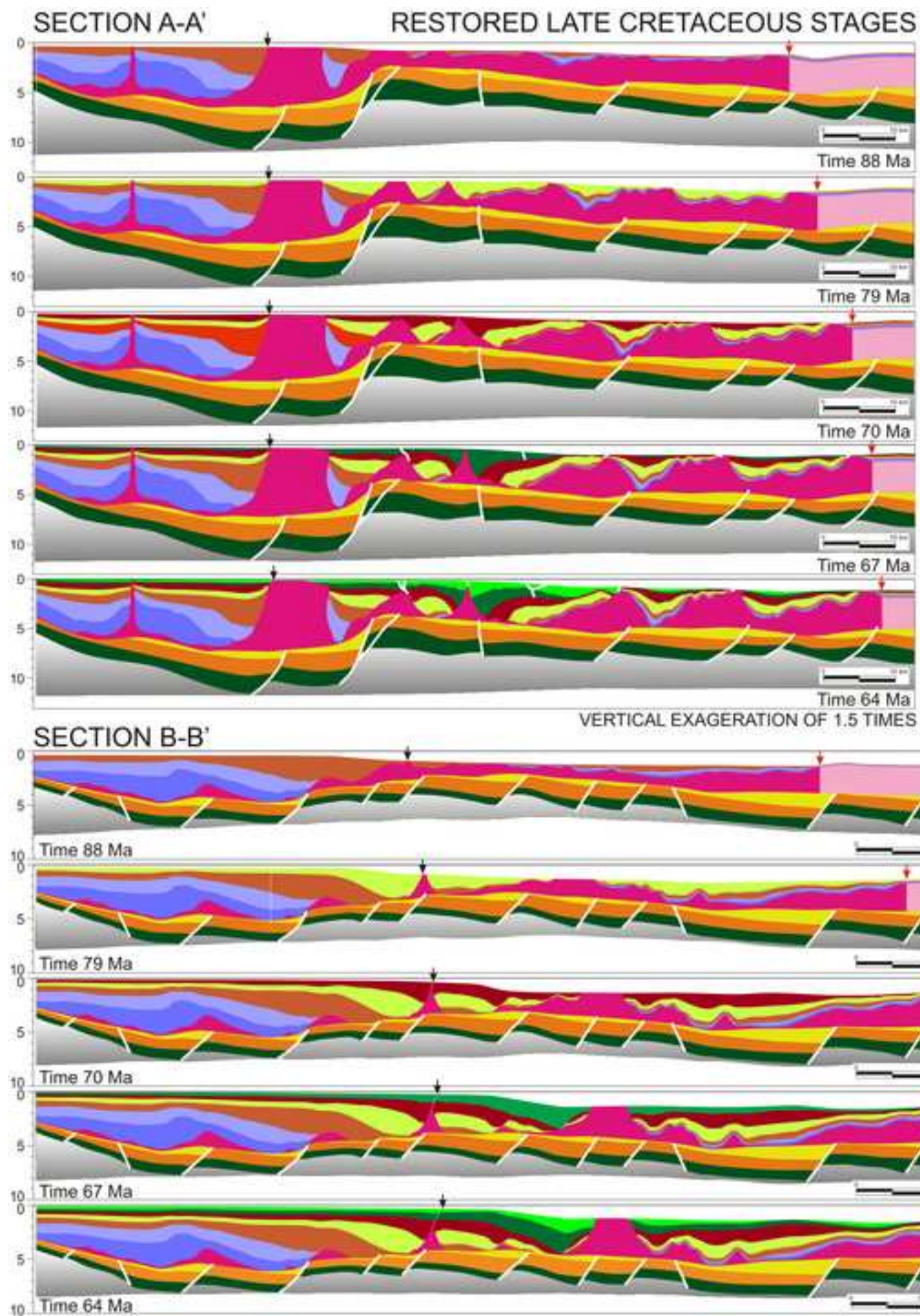


Figure 13
[Click here to download high resolution image](#)

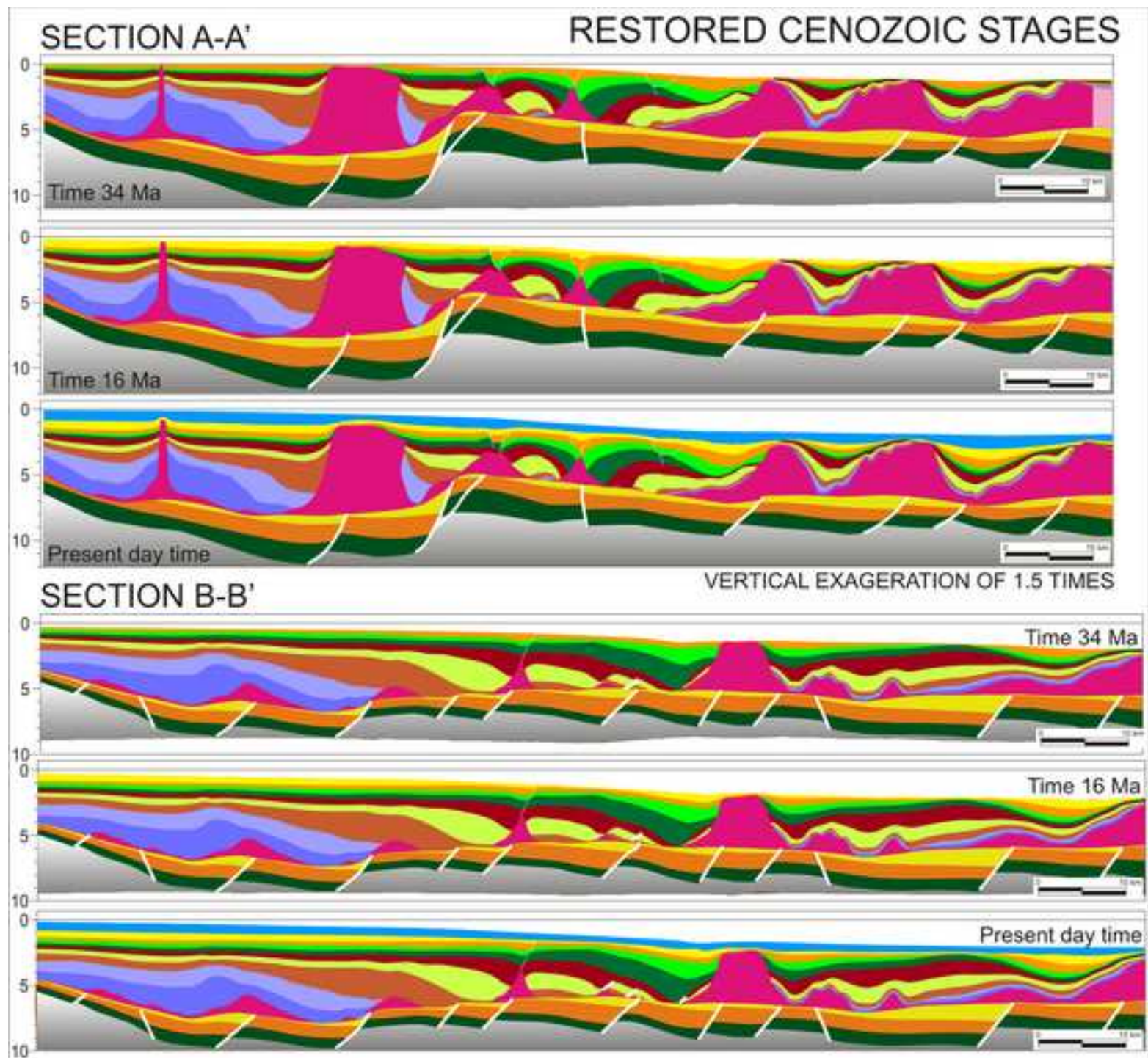


Figure 14
[Click here to download high resolution image](#)

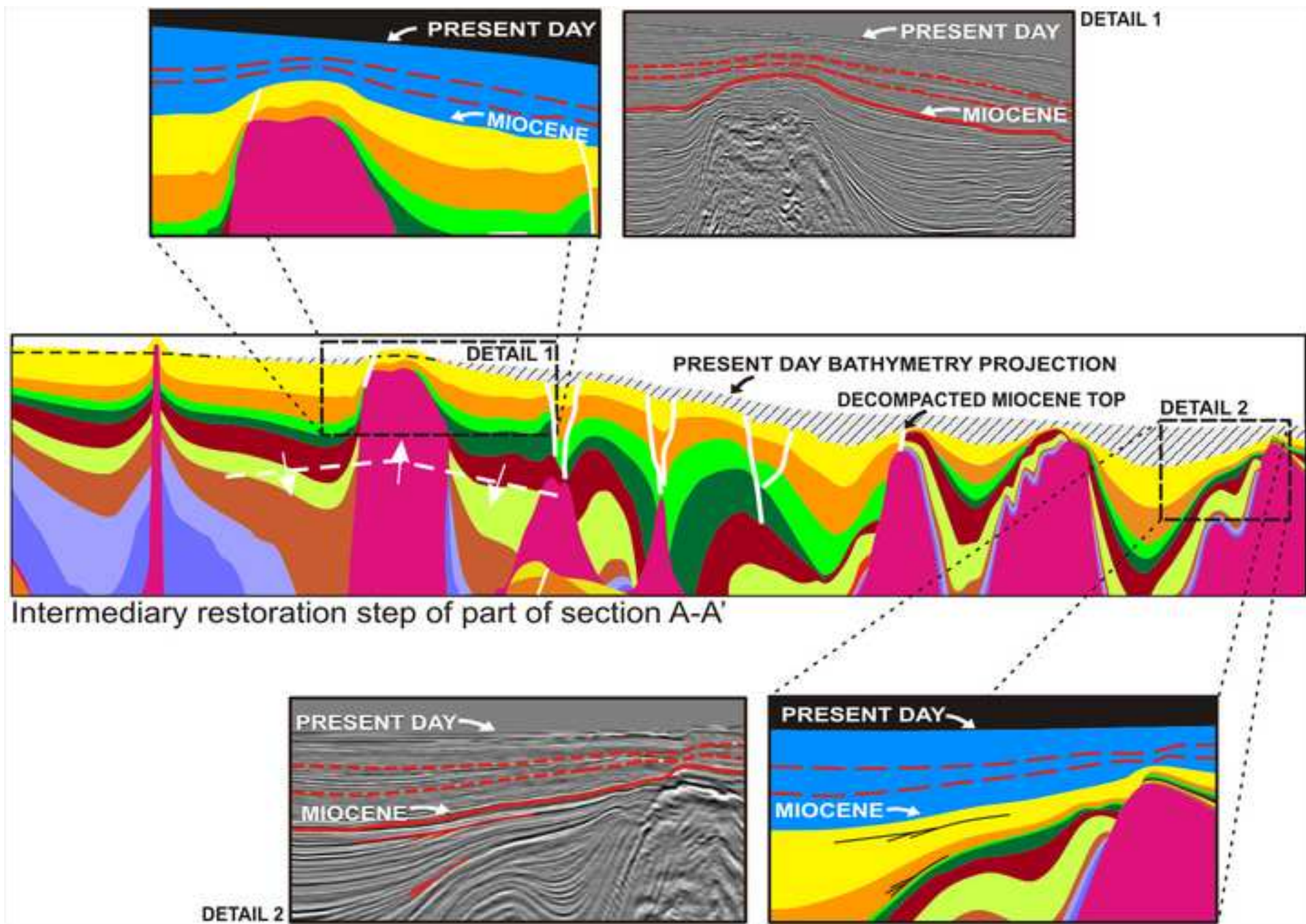


Figure 15
[Click here to download high resolution image](#)

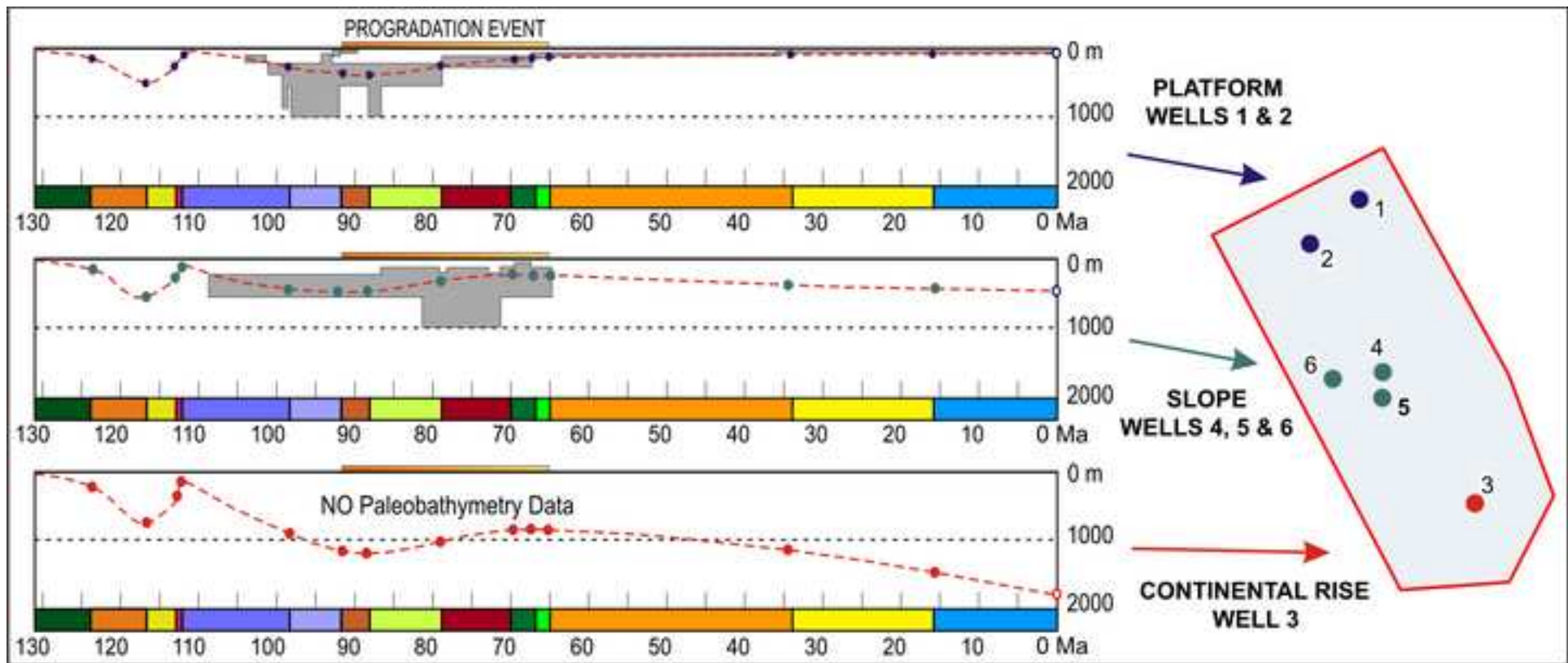


Figure 16
[Click here to download high resolution image](#)

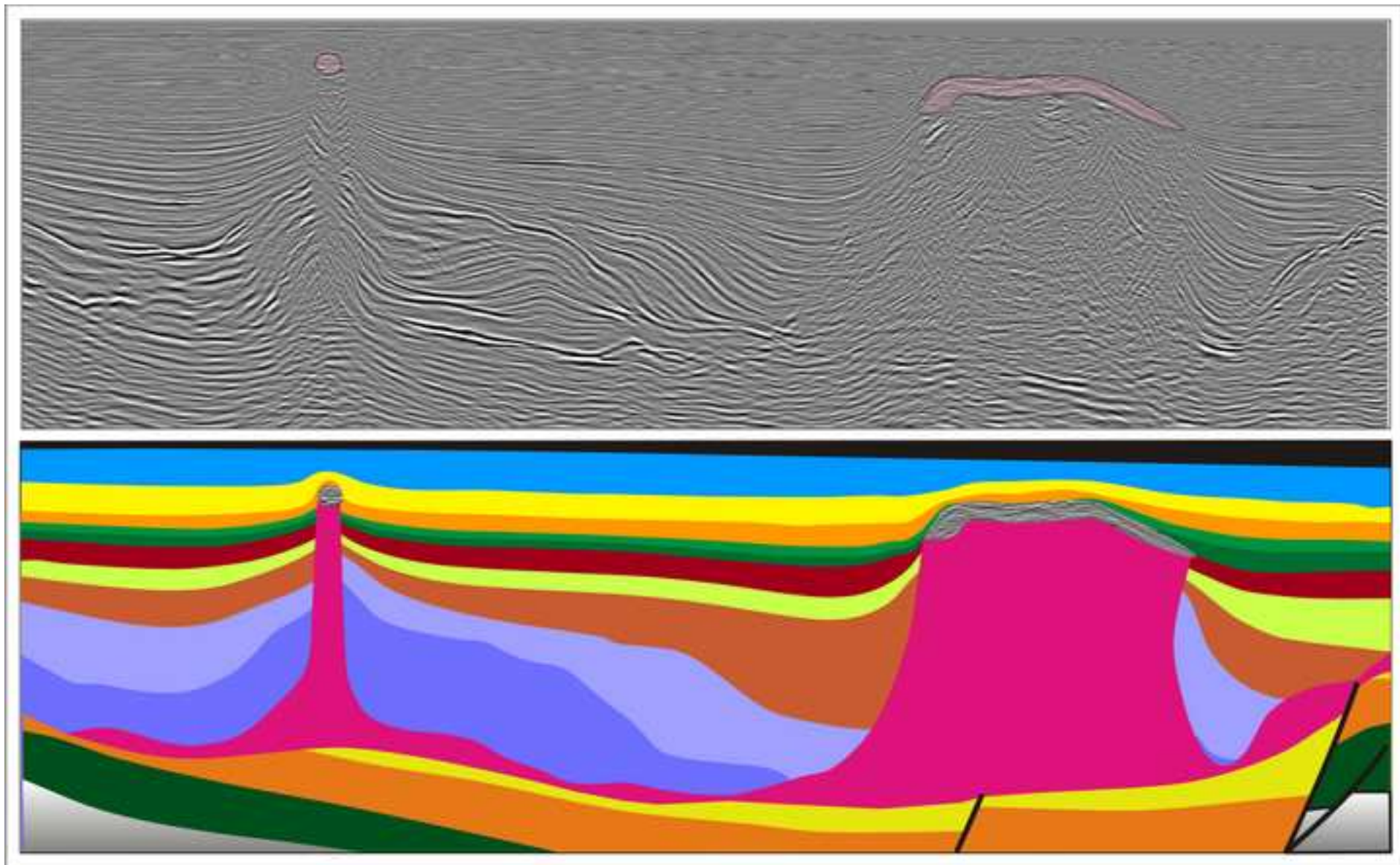
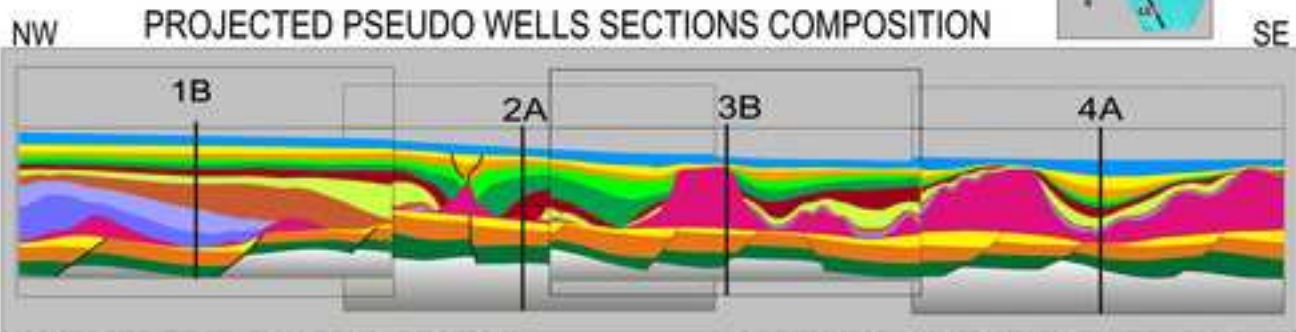


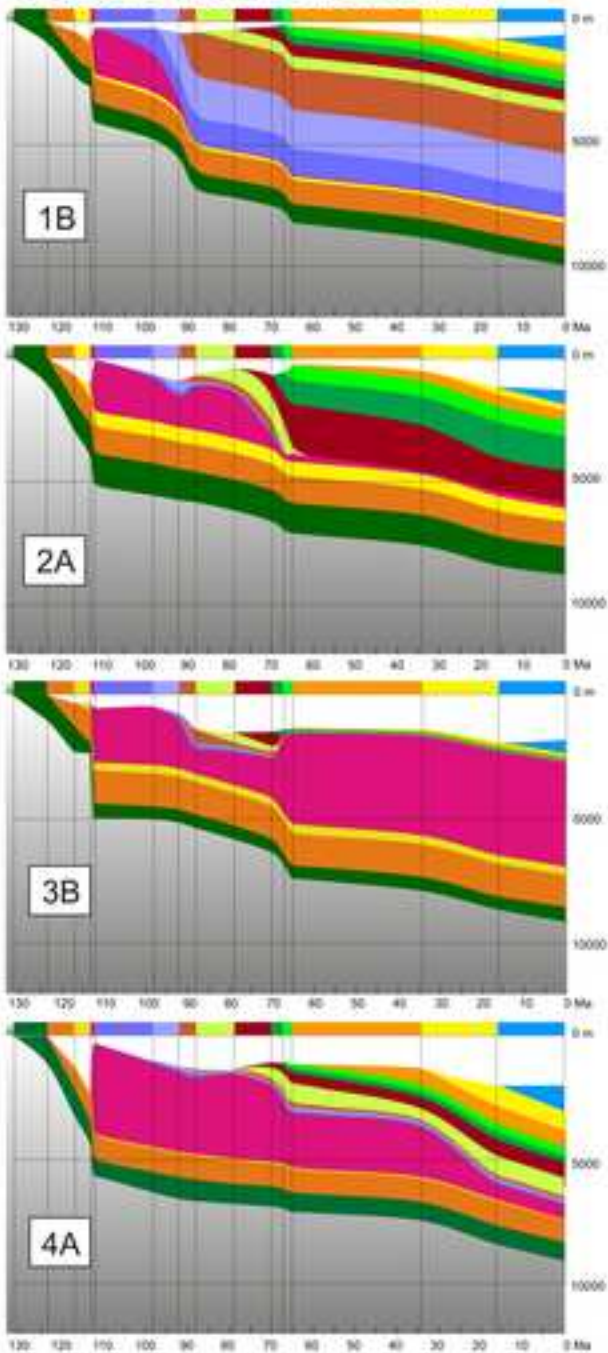
Figure 17

[Click here to download high resolution image](#)

PSEUDOWELLS 1D ANALYSIS



SUBSIDENCE GEOHISTORY



OVERBURDEN GEOHISTORY

